

---

# Federated Variational Inference for Bayesian Mixture Models

---

Jackie Rao<sup>1</sup> Francesca L. Crowe<sup>2</sup> Tom Marshall<sup>2</sup> Sylvia Richardson<sup>1</sup> Paul D. W. Kirk<sup>1</sup>

## Abstract

We present a federated learning approach for Bayesian model-based clustering of large-scale binary and categorical datasets. We introduce a principled ‘divide and conquer’ inference procedure using variational inference with local merge and delete moves within batches of the data in parallel, followed by ‘global’ merge moves across batches to find global clustering structures. We show that these merge moves require only summaries of the data in each batch, enabling federated learning across local nodes without requiring the full dataset to be shared. Empirical results on simulated and benchmark datasets demonstrate that our method performs well in comparison to existing clustering algorithms. We validate the practical utility of the method by applying it to large scale electronic health record (EHR) data.

## 1. Introduction

Federated learning (FL) refers to the setting in which a network of clients collaboratively train a model, while ensuring that the training data are kept local (Kairouz et al., 2021). FL was introduced as a way to enable learning when datasets are large and/or privacy sensitive (McMahan et al., 2017). There have been numerous developments in supervised FL, but methods for unsupervised FL remain limited (Tian et al., 2024). While a number of federated clustering algorithms have been proposed (e.g. federated  $k$ -means: Kumar et al., 2020; Liu et al., 2020; Garst & Reinders, 2025), and Bayesian FL (BFL) is an active area of research (see Cao et al., 2023, for a survey), we are not aware of previous studies into FL for Bayesian model-based clustering, which we consider here.

Mixture models provide a probabilistic approach for clustering by assuming data are generated from a mixture of underlying probability distributions. Bayesian mixture mod-

els enable the uncertainty in cluster allocations and, potentially, the number of clusters to be modelled. These include Bayesian finite mixture models (e.g. Diebolt & Robert, 1994; Richardson & Green, 1997; Rousseau & Mengersen, 2011), as well as Bayesian nonparametric methods, such as Dirichlet process (DP) mixture models (Ferguson, 1973; Escobar & West, 1995). Markov Chain Monte Carlo (MCMC), particularly Gibbs sampling (Neal, 2000), is often used to draw samples from the intractable posterior (e.g. Robert & Casella, 2004; Walker, 2007). Despite efforts to improve scalability, MCMC algorithms are often too computationally intensive for even moderately large datasets, and/or may experience mixing issues, preventing the sampler from reaching convergence (Celeux et al., 2000).

To address the growth of ‘massive’ datasets, a range of methods have been proposed to scale MCMC algorithms to large sample sizes (e.g. Huang & Gelman, 2005). These include distributed computing approaches in which the computational and memory requirements of an algorithm are split, with the algorithm running in parallel on multiple nodes (Zhu et al., 2017). An important example of this for Bayesian inference is *consensus Monte Carlo*, where a Monte Carlo algorithm is run on partitions of the data and samples are then aggregated across partitions to enable ‘global’ inferences to be drawn (Scott et al., 2016). Various methods have been proposed to aggregate the subset posteriors. Informally, the challenge for clustering models is how to match clusters/cluster labels across data partitions. The SNOB (Zuanetti et al., 2018) and SIGN (Ni et al., 2019) algorithms have been proposed to address this.

Distributed variational inference (VI) algorithms have also been proposed to obtain an approximation of the posterior distribution, including variational consensus Monte Carlo (VCMC) (Rabinovich et al., 2015). As noted in Rabinovich et al. (2015), models with unidentifiable latent variables, such as component allocation labels in mixture models, present additional complexity for such approaches, and the authors suggested a heuristic approach using the Hungarian algorithm (Kuhn, 1955) to align cluster centres across data partitions. Our proposed method instead utilises the variational objective function to allow us to combine results from data partitions in a statistically principled manner.

While VI methods tend to have better run-time performance than MCMC algorithms (e.g. Blei et al., 2017), they can also

---

<sup>1</sup>MRC Biostatistics Unit, University of Cambridge, Cambridge, United Kingdom <sup>2</sup>Institute of Applied Health Research, University of Birmingham, Birmingham, United Kingdom. Correspondence to: Jackie Rao <jackie.rao@mrc-bsu.cam.ac.uk>.

be sensitive to initialisation due to local optima in the objective function. To address these issues when fitting mixture models, ‘merge’ and ‘delete’ moves may be incorporated into the variational algorithm to dynamically combine or remove unnecessary clusters. Such moves, in addition to ‘split’ moves to create new clusters, have been seen to improve inference in expectation-maximisation (EM) algorithms (Ueda et al., 2000) and MCMC samplers (Jain & Neal, 2004; Dahl & Newcomb, 2021) for mixture models, and have also been employed less commonly in VI algorithms for DP mixtures, including Gaussian DP mixture models (Hughes et al., 2015; Lin, 2013), and the hierarchical DP (Hughes & Sudderth, 2013).

Here we propose a distributed algorithm that performs inference for Bayesian mixture models using VI with local merge and delete moves within batches of the data across a network of nodes in parallel, followed by ‘global’ merge moves to aggregate clusters across batches. We show that these ‘global’ moves require only summaries of the data from each node, enabling federated learning of the model without requiring the full dataset to be shared. We anticipate that the approach may be useful for the analysis of privacy sensitive datasets, and provide an example application clustering individual-level electronic health records (EHRs).

We focus on applications to categorical, particularly binary (2-category) datasets, but note that our approach can be straightforwardly adapted to mixtures of Gaussians and other members of the exponential family. In Section 2, we provide an overview of variational Bayesian mixture models, and in Section 3 we briefly introduce merge/delete moves. Section 4 describes how we can employ these moves to enable scaling to large datasets and federated learning. Sections 5 and 6 present results from both simulated and real-world data, including a British EHR dataset, and we discuss the results and take a brief look at future directions for the model in Section 7. We consider in the Appendix how our model can be extended to tackle variable selection.

## 2. Model Overview

### 2.1. Bayesian Finite Mixture Models

Let  $X = \{x_1, \dots, x_N\}$  denote the observed data, where  $x_n$  is one observation of  $P$  categorical variables. We model the generating distribution as a finite mixture of  $K$  components. Each observation is generated by one component. The general equation for a  $K$  component finite mixture model is:

$$p(X|\pi, \phi) = \sum_{k=1}^K \pi_k f(X|\phi_k), \quad (1)$$

where component densities  $f(X|\phi_k)$  are usually from the same parametric family but with different parameters as-

sociated with each component. In the limit as  $K$  goes to infinity, this is equivalent to the Dirichlet process (DP) mixture model (Maceachern, 1994; Escobar & West, 1995). Our model can be seen as a finite truncation of the DP mixture model to allow for simpler inference, setting  $K$  to be larger than the number of clusters we expect. Each component is modelled as a categorical distribution across  $P$  covariates with parameters  $\phi_{kj} = [\phi_{kj1}, \dots, \phi_{kjL_j}]$ , where  $\phi_{kjl}$  represents the probability that variable  $j$  takes value  $l$  in component  $k$ .  $L_j$  is the number of categories for variable  $j$ . The mixture weight for the  $k$ -th component is denoted by  $\pi_k$ , satisfying  $\sum_{k=1}^K \pi_k = 1$  and  $\pi_k \geq 0$ .

We introduce latent variables  $z_n$  associated with each  $x_n$ , such that each  $z_n$  is a one-hot-encoded binary vector with  $z_{nk} = 1$  if and only if  $x_n$  is in the  $k$ -th cluster. We then rewrite Equation (1) as:

$$p(X|Z, \pi, \phi) = \prod_{n=1}^N \prod_{k=1}^K f(x_n|\phi_k)^{z_{nk}}. \quad (2)$$

To complete the model specification for the Bayesian model, we place priors on the parameters:

$$\pi = (\pi_1, \dots, \pi_K) \sim \text{Dirichlet}(\alpha_0), \quad (3)$$

$$\phi_{kj} = (\phi_{kj1}, \dots, \phi_{kjL_j}) \sim \text{Dirichlet}(\epsilon_j), \quad (4)$$

where all Dirichlet priors are symmetric. It has been shown theoretically that if  $K$  exceeds the true number of clusters, then, under certain assumptions, setting  $\alpha_0 < 1$  in Equation (3) allows the posterior to asymptotically converge to the correct number of clusters as the number of observations goes to infinity (Rousseau & Mengersen, 2011; van Havre et al., 2015; Malsiner-Walli et al., 2014). Further details of hyperparameter settings are provided in the Appendix. The model can be extended to simultaneously tackle variable selection, as in (Law et al., 2004) and (Tadesse et al., 2005), which is explored in the Appendix.

### 2.2. Mean-Field Variational Inference (VI)

We employ a variational inference (VI) approach to seek an approximate distribution  $q$  to the posterior. We optimise the Evidence Lower Bound (ELBO) given below,  $\mathcal{L}(q)$ , with respect to  $q(\theta)$ , where  $\theta$  is a collection of all parameters in the model.

$$\mathcal{L}(q) = \int q(\theta) \ln \left( \frac{p(X, \theta)}{q(\theta)} \right) d\theta \quad (5)$$

This is equivalent to minimising the Kullback-Leibler (KL) divergence between  $q(\theta)$  and the true posterior,  $p(\theta|X)$ . We constrain  $q$  to be a mean-field approximation which can be fully factorised as:  $q(\theta) = q_Z(Z)q_\pi(\pi)q_\Phi(\Phi)$ . We use a standard variational EM algorithm to optimise  $\mathcal{L}(q)$  (see, for example, Bishop, 2006), as described below.

**‘E’ Step** We update the latent variables  $Z$  with the current variational distributions of all other parameters.

$$q^*(Z) = \prod_{n=1}^N \prod_{k=1}^K r_{nk}^{z_{nk}}, \quad r_{nk} = \frac{\rho_{nk}}{\sum_{j=1}^K \rho_{nj}} \quad (6)$$

$$\ln \rho_{nk} = \mathbb{E}_\pi[\ln \pi_k] + \sum_{i=1}^P \mathbb{E}_\Phi[\ln \phi_{kix_{ni}}] \quad (7)$$

$r_{nk}$  is the responsibility of the  $k$ -th component for the  $n$ -th observation, and  $\mathbb{E}[z_{nk}] = r_{nk}$ .

**‘M’ Step** Given updated responsibilities  $r_{nk}$  in the ‘E’ step, we then update cluster-specific parameters:

$$q^*(\pi) = \text{Dirichlet}(\alpha_1^*, \dots, \alpha_K^*) \quad (8)$$

$$q^*(\phi) = \prod_{k=1}^K \prod_{j=1}^P \text{Dirichlet}(\epsilon_{kj1}^*, \dots, \epsilon_{kjL_j}^*) \quad (9)$$

where for  $k = 1, \dots, K, j = 1, \dots, P, l = 1, \dots, L_j$ :

$$\alpha_k^* = \alpha_0 + \sum_{n=1}^N r_{nk} \quad (10)$$

$$\epsilon_{kjl}^* = \epsilon_{jl} + \sum_{n=1}^N \mathbb{I}(x_{nj} = l) r_{nk} \quad (11)$$

Expectations throughout are taken with respect to variational distributions. Between each ‘E’ and ‘M’ step, we calculate the value of the ELBO and use this to monitor convergence. All values are initialised using k-modes (Chaturvedi et al., 2001), a method analogous to k-means for categorical data.

### 3. Variational Merge/Delete Moves

As in eg. (Hughes et al., 2015), we introduce merge and delete moves which can be integrated into the VI algorithm. Merge moves refer to moves that combine observations from two clusters into one unified cluster; delete moves refer to moves to delete unnecessary extra clusters in the model. Both moves enable redundant clusters to be efficiently removed to help the model to escape local optima, and are designed in a principled manner to align with the ELBO variational objective function.

When moves are proposed, parameters in the VI framework are updated through initially updating responsibilities,  $r_{nk}$ , which are directly associated with the cluster assignment of observations, and then following through with classical variational EM steps. Moves are only accepted if they improve or maintain the ELBO, otherwise the original configuration is maintained, ensuring that the method remains consistent with the underlying VI framework.

Variational implementations of these moves in Dirichlet process mixture models, in addition to split moves, have been shown to outperform standard variational Bayes and related algorithms (Hughes et al., 2015; Yang et al., 2019). However, little work has been published regarding variational categorical mixture models. In particular, split moves are not relevant in the overfitted finite mixture model setting. We provide clear, practical strategies for the implementation of these moves in the categorical setting in Appendix E.

In particular, we consider how candidate clusters for merge and delete moves can be chosen to enhance efficiency in categorical mixture models. Comparing ELBOs between all possible merge/delete proposals would result in an unnecessarily high computational cost. We demonstrate through simulations in Appendix J.4 that using fast-to-calculate heuristics such as correlation between cluster parameters (when proposing to merge) allows for enhanced efficiency and a higher percentage of accepted merge moves compared to randomly selecting candidate clusters. This aspect has rarely been explored in prior research.

#### 3.1. Computational Considerations

We name the variational algorithm including merge/delete moves ‘MerDel’ and introduce a parameter, ‘laps’, representing how many variational EM cycles we go through before performing a merge and a delete move.

Both merge and delete moves include some variational E and M steps to reassign observations to new clusters as described in Appendix E. These merge/delete moves are therefore relatively costly if the move is ultimately rejected, as opposed to doing purely variational steps which are guaranteed to improve the ELBO. As the model approaches convergence, more variational moves are needed to fine-tune cluster assignments while merge/delete proposals are rejected and increase overall computation. There is subsequently a trade-off between proposing more merge/delete moves to allow for bigger, more effective moves earlier on in MerDel versus reducing the amount of ‘wasted’ moves as the model approaches convergence, which we examine further in simulations. One method to mitigate this in future could be to dynamically change the ‘laps’ parameter as merges/deletes are more frequently rejected.

#### 3.2. Parallelising MerDel

VI requires fewer sweeps over the dataset to perform inference compared to MCMC samplers, and is feasible for datasets with thousands of observations. This allows variational mixture models to be more computationally efficient and converge quickly, especially with the addition of merge/delete moves allowing models to avoid getting stuck in local optima. Despite these improvements, VI still reaches computational bottlenecks when  $N$  is particularly

large; we see in simulations later that MerDel is infeasible as we reach datasets with  $N$  of order  $10^5$ . Repeatedly updating  $N \times K$  responsibilities every E step, and subsequently summing these over  $N$  to update cluster-specific parameters every M step is computationally costly once  $N$  is large, even if there are 100s of iterations compared to the 1000s seen in MCMC.

All individual components of the original algorithm can be parallelised using standard methods. For example, in the E step, calculation of responsibilities  $r_{nk}$  can be parallelised over  $n$ . Summations in the M step can also be parallelised. We provide an implementation of such a parallelised VI as part of this manuscript.

However, the overall algorithm is not embarrassingly parallel; for example,  $r_{nk}$  values for all  $N$  observations are required to update cluster-specific parameters for a given cluster  $k$ . Prior literature has consistently highlighted the limited gains achieved by such partial parallelisation for iterative methods such as VI. This is due to the significant computational overhead incurred when feeding intermediate results to and from one ‘master’ core - a globally shared computation unit - at regular, frequent intervals (Nallapati et al., 2007; Neiswanger et al., 2015). Nallapati et al. in particular saw that when parallelising variational E and M steps in Latent Dirichlet Allocation, the gain in efficiency was not significant due to the read-conflict between various threads, and also raised concerns about memory constraints as the whole dataset was stored in memory (2007).

## 4. Federated Variational Inference

In this section, we propose a scalable clustering algorithm for large categorical datasets, FedMerDel (Federated MerDel), which addresses the challenge of large  $N$  and enables federated learning across multiple nodes.

In FedMerDel, we use a ‘divide and conquer’ inference procedure. We assume our dataset has been split into  $B$  ‘batches’ - these batches will already be pre-determined if subsets of the data are held by separate parties, or may be artificially created by random partitioning of the data. The first ‘local’ step of the algorithm involves carrying out clustering via MerDel in each data batch separately. The size and number of these batches should be chosen so inference is computationally feasible; pre-existing subsets of the data can be divided further if necessary. Each batch is processed in parallel, and the clusters produced are referred to as ‘local clusters’.

The second ‘global’ step then combines the local clustering structures. Local clusters are frozen, and we merge similar local clusters into ‘global’ clusters. This is conceptually similar to approaches used in SNOB (Zuanetti et al., 2018) and SIGN (Ni et al., 2019), but both use MCMC methods which are computationally costly; local clustering in SNOB takes

over 4 hours for a batch of size  $N = 1000$  in the authors’ simulations. We utilise a version of the variational merge move seen in MerDel to implement a ‘global merge’. By freezing local clusters in the global merge, the proposed clustering structure and ‘global ELBO’ across all observations can be efficiently calculated by utilising stored parameter values. The variational framework allows us to accept or reject global merges in a principled manner. Importantly, the full dataset is not required in the global merge.

In contrast to the approach considered in Section 3.2, instead of optimising individual components of the existing classical variational algorithm, our approach is designed to present a scalable clustering model which avoids these bottlenecks entirely by adopting a distributed computing approach in which each data batch is analysed independently and in parallel before ‘global merge’ steps are used to obtain a (global) mixture model for the full dataset. This federated learning approach eliminates the need for frequent communication and synchronization during the main variational updates, while data remains decentralised.

### 4.1. Estimating Global Clusters

Assume our data has been split into  $B$  batches and MerDel has been run on each batch, with  $K_b$  local clusters in Batch  $b$ . Let  $K = \sum_{b=1}^B K_b$  be the total number of local clusters. We assume we are in the setting with no variable selection. In the global step, we first ‘combine’ all our existing variational parameters from each batch. For  $q(\pi)$ , we concatenate all our  $K_b$ -length  $\alpha$  vectors to one  $K$ -length  $\alpha$  vector. Each  $q(\phi_{kj})$  is already independent for each local cluster  $k$  (and each covariate  $j$ ). We create a new matrix of responsibilities  $r_{nk}$  as an  $N \times K$  block diagonal matrix, consisting of blocks of  $N_b \times K_b$  responsibility matrices from each batch.  $\sum_{k=1}^K r_{nk} = 1$  still holds for all  $n$ .

Let clusters  $k_1$  and  $k_2$  be considered for a merge. As in the local merge, we reassign responsibilities to cluster  $k_1$  via  $r_{nk_1}^{new} = r_{nk_1} + r_{nk_2}$  for all  $n = 1, \dots, N$ . This can be viewed as summing columns  $k_1$  and  $k_2$  in our responsibility matrix. We then use the definitions of  $\alpha^*$ ,  $\epsilon^*$  (Equations (10), (11)) as follows to update cluster-specific parameters:

$$\alpha_{k_1}^{new} = \alpha_0 + \sum_{n=1}^N (r_{nk_1} + r_{nk_2}) \quad (12)$$

$$= \alpha_{k_1}^* + \alpha_{k_2}^* - \alpha_0 \quad (13)$$

$$\epsilon_{k_1 j l}^{new} = \epsilon_{j l} + \sum_{n=1}^N \mathbb{I}(x_{nj} = l) (r_{nk_1} + r_{nk_2}) \quad (14)$$

$$= \epsilon_{k_1 j l}^* + \epsilon_{k_2 j l}^* - \epsilon_j \quad (15)$$

This avoids calculating sums over  $N$ . To complete the merge, we remove all parameters associated with cluster  $k_2$  -  $\alpha_{k_2}^*$ ,  $\epsilon_{k_2 j}^*$  and  $r_{nk_2}$  for all  $n = 1, \dots, N$ ,  $j = 1, \dots, P$ .

Unlike the variational merge moves, we do not perform an extra variational E/M step to allow observations to move in and out of the new cluster. This would require a whole-dataset update of responsibilities  $r_{nk}$ . The efficiency of the global merge hinges on the fact that local clusters are frozen. We propose global merge candidates in two ways; a greedy search and a random search.

**Greedy Search** We prevent merges between two clusters from the same batch with a greedy search, on the hypothesis that such merges would already have taken place at the local stage. This can be carried out in a sequential manner by examining the correlation/divergences between Cluster 1 of Batch 1 and all clusters in Batch 2. Once Cluster 1 has merged with any cluster in Batch 2, we move to Batch 3 and consider merging with the clusters in this batch. We repeat for all batches, before moving to Cluster 2 of Batch 1 and so on until we have gone through all clusters in Batch 1. We then repeat the process with Batches 2, 3, ..., B, looking only at Batches  $b + 1, \dots, B$  for Batch  $b$ .

**Random Search** Similarly to local merge moves, we calculate correlations/divergences between all  $K$  clusters, and pick the merge candidate pair randomly between the 3 pairs with the highest correlation (provided correlation  $> 0.05$ ) or lowest divergence. There is no restriction on proposing merges between two clusters of the same batch. This stops after a fixed number of global merge moves (e.g. 10) have been rejected consecutively.

## 4.2. Efficient Global ELBO Calculation

The ELBO variational objective function allows us to accept or reject the global merge under a rigorous probabilistic framework. For the global merge to be accepted, the ELBO must be higher in the new, merged model. As we now consider the full dataset, many terms in the overall ELBO function involve all observations and clusters. ‘Freezing’ local clusters allows us to efficiently calculate the majority of the ELBO terms while enabling the model to handle large-scale data. Two sums involving  $N$  in the full ELBO function can be written as a sum over smaller  $K, P, L_j$  of sufficient statistics which can in turn be calculated as a linear function of previously calculated  $\alpha^*$  and  $\epsilon^*$ :  $T_k = \sum_{n=1}^N r_{nk} = \alpha_k^* - \alpha_0$  and  $S_{kjl} = \sum_{n=1}^N r_{nk} \mathbb{I}(x_{nj} = l) = \epsilon_{kjl}^* - \epsilon_{jl}$ . This vastly reduces the number of operations required.

The final term involving  $N$  is an assignment entropy term,  $\sum_{n=1}^N \sum_{k=1}^K r_{nk} \ln r_{nk}$ , which is not linear in any previously calculated parameters. This is additive over  $N$  and  $K$ , so we can calculate this value separately for each batch (in parallel if required) before adding all results together. However, in our greedy search where we never combine two clusters from the same batch,  $r_{nk_1}$  and/or  $r_{nk_2}$  will *always* be zero for any merge, for all  $n = 1, \dots, N$ . Observation  $n$  is

only explained by clusters originating from certain batches of data and a merge is only proposed from a new batch where  $n$  is not explained by any clusters associated with that batch. This allows greedy search to be faster, although merges could potentially be missed.

Full details of the global ELBO calculation can be found in Appendix F, where all terms in the ELBO can be written without  $X$ . Crucially, the global merge move allows us to seek a clustering structure for the full dataset without any scan over the full data matrix  $X$ , which is essential for federated learning. Data from separate entities remains decentralised, where only statistics from each batch are required to be shared, allowing for increased data security and privacy. We also note that parallelisation in local batches, as in Section 3.2, could still be applied to FedMerDel for additional gains, given sufficient computational resources.

## 4.3. Implementation

The model builds upon an existing R package, VICatMix (Rao & Kirk, 2024), which applies VI for binary and categorical Bayesian finite mixture models (with no merge/delete moves). Rcpp and RcppArmadillo are used to accelerate computation with C++. MerDel runs on a single-core processor, where, for example, inference for a mixture model fitted to a binary dataset of size  $N = 2000, P = 100$  generally converges in less than a minute.

FedMerDel allows MerDel to be run independently on a different core per batch of data; a subsequent global merge takes only a few seconds at most in all simulations. Reported ‘wall-clock times’ take this parallelisation into account where clearly stated. Simulations were all run on a university multi-core HPC cluster.

## 5. Examples

### 5.1. Simulation Study

In this section, all simulated data is binary, with the data generating mechanism detailed in the Appendix. Additional simulation studies comparing merge criteria, looking at scenarios with simulated categorical data with 3+ categories, and looking at variable selection can also be found in the Appendix.

**Frequency of Merge/Delete Moves** In Section 3.1, we described the trade-off between more or fewer merge/delete moves in MerDel. We ran simulation studies comparing different values of the parameter ‘laps’ representing the frequency of merge/delete moves in a run of MerDel, with  $\text{laps} \in \{1, 2, 5, 10\}$ . We also compared to a model with just merge/delete moves after performing one ‘E’ and ‘M’ step after initialisation (‘laps = 0’), and the variational model with no merge/delete moves (‘laps = 10000’). We used

correlation for merge criteria.

We compared computational efficiency by measuring the wall-clock time taken for convergence. We additionally compared the number of non-empty clusters found, and the Adjusted Rand Index (ARI) with the simulated ‘true’ labels. Details of the simulated datasets are in Appendix I.3.

**Global Merge Simulations** We evaluated the clustering performance when splitting data into batches and performing a global merge as detailed in Section 4, and compared this with the performances of MerDel applied to the full dataset, and parallelised MerDel as described in Section 3.2. We looked at binary data with sizes varying between  $N =$  between 10,000 to 1,000,000 with  $P = 100$  covariates, and additional simulations varying  $P$  and looking at categorical data in the Appendix. Full details are in Appendix I.4.

**Number of Batches** With datasets of size  $N = 100,000$  and  $N = 200,000$ , we compared the clustering performance when considering different numbers of batches. Further details are in Appendix I.5.

## 5.2. MNIST

We applied our model to the MNIST collection of  $N = 60000$  images of handwritten digits 0-9 (LeCun et al., 2011). As in Mansinghka et al. (2016), we downsampled each image to  $16 \times 16$  pixels using bilinear interpolation via TensorFlow, and represented this as a 256-dimensional binary vector. Furthermore, to reduce computation on irrelevant pixels (e.g. those in corners of the image) we removed all pixels with fewer than 100 non-zero values across the whole dataset, leaving 176 covariates. We split this into 6 batches of  $N = 10000$  and set  $K = 20$  as the maximum clusters in each batch. True labels for the MNIST digits were not used at any point in the unsupervised clustering.

## 5.3. Electronic Health Record (EHR) data

We analysed an anonymised EHR dataset derived from The Health Improvement Network (THIN) database that comprised records from 289,821 individuals in the United Kingdom over the age of 80. For 94 long-term health conditions, we recorded which conditions were present in each individual to create a  $289,821 \times 93$  binary matrix whose  $(i, j)$ -entry indicates whether individual  $i$  has condition  $j$  (encoded as a 1) or not (encoded as 0). Further details on data preprocessing are provided in Appendix L. The aim of the analysis is to identify clusters of individuals with common patterns of co-occurring conditions (multimorbidity).

## 6. Results

### 6.1. Simulation Study

#### 6.1.1. FREQUENCY OF MERGE/DELETE

More detailed results for simulations, including an assessment of the quality of variable selection with noisy data, can also be found in Appendix J.1. The main conclusions of the simulation study are as follows:

**Incorporating merge/delete enables faster convergence in terms of wall-clock time:** Generally, MerDel models are faster to converge. Figure S1 in Appendix J.1 shows that early accepted merge/delete moves allow for substantial early increases in the ELBO. However, as described in Section 3.1, there is a trade-off that must be made - models with laps = 1, for example, get close to convergence very fast but then take more time to fully converge. The inclusion of frequent merge/delete moves at the start of the algorithm can also lead to the algorithm jumping to a worse local optimum, reflected in slightly lower ARIs in some cases.

**Better ARIs are achieved with merge/delete:** Figure 1 and Appendix J.1 show that (especially in Simulations 1.1, 1.2 and 1.3) using laps = {2, 5, 10} generally allows for models with higher ARIs than the variational model with no merge/delete moves.

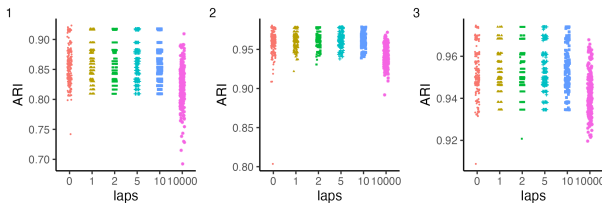


Figure 1. Scatter plot comparing ARIs achieved by each model across all datasets and initialisations in Simulations 1.1, 1.2 and 1.3 (labelled 1, 2, 3 respectively). Each point represents one ARI from one MerDel run.

**Merge/delete more accurately estimates the number of clusters:** The model with no merge/delete moves tends to vastly overestimate the number of true clusters in the data due to the existence of small unnecessary clusters. MerDel mitigates this, with Figure S2 in Appendix J.1 showing that the model often is able to find the exact true number. Some sporadic small clusters remain when implementing merge/delete moves every 10 laps in Simulation 1.3, indicating we could need more frequent moves as  $N$  increases.

**Variational moves are still necessary:** The algorithm with purely merge/delete moves performs less well; any result of this algorithm is extremely dependent on initialisation. Observations can never move between two clusters.

### 6.1.2. GLOBAL MERGE SIMULATIONS

Results for selected simulations with  $N$  ranging from 50,000 to 500,000 can be seen in Table 1, with further results in Appendix J.2. In our simulations, we compare to the ‘‘gold standard’’ setting in which the full dataset may be analysed without batching using MerDel with or without parallelisation (denoted by ‘par’ and ‘full’ in our results tables). We see from Table 1 that FedMerDel gave extremely good clustering results with median ARIs only marginally lower than those for ‘full’ and ‘par’.

The time taken was substantially faster for both parallelised MerDel and FedMerDel as expected via distributed computing, where MerDel on the full dataset became infeasible as our data sizes became larger due to the computational requirements of manipulating large matrices. However, as hypothesised in Section 3.2, we saw that FedMerDel was faster than parallelised MerDel, and became substantially more so as  $N$  increased (Figure 2). Global merge times ranged from a mean of 0.29s(greedy)/0.39s(random) for  $N = 20,000$  to a mean of 14.8s(greedy)/18.2s(random) for  $N = 500,000$ , showing that the time taken for the global merge was not computationally prohibitive.

Different batches of data for a dataset provided extremely consistent results, eg. the standard deviation of ARIs across 10 different shuffles of data in an  $N = 50,000$  simulation ranged from 0.0003 to 0.005 for the 20 simulated datasets. Notably, even if a cluster resides in only one batch of data, there is no requirement in our algorithm for this cluster to merge with clusters from other batches (if it does not improve the ELBO), allowing our algorithm to hold sound for data which is not identically distributed across partitions.

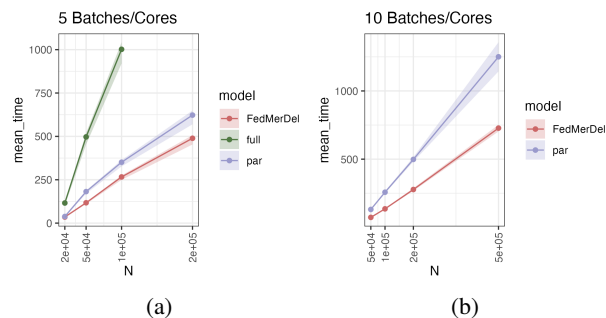


Figure 2. Plot comparing the mean time taken by MerDel with and without parallelisation (‘par’ and ‘full’), and FedMerDel as we vary  $N$  with 5 or 10 batches/cores in ‘Global Merge Simulations’, with an approximate 95% confidence interval (mean  $\pm 1.96 \times \frac{s.d.}{\sqrt{n}}$ ). Results for FedMerDel are with the random search.

### 6.1.3. NUMBER OF BATCHES

We saw that as we increased the number of batches used, although there was no statistically significant difference at

the 5% level in the accuracy of the clustering as measured by ARI, we did see more clusters (Appendix J.3). Nevertheless, ARI values were all above 0.93 with a mean of 0.957 across all simulations.

## 6.2. MNIST

We ran FedMerDel on 5 different ‘shuffles’ of the data into batches with  $K = 20$  maximum clusters in each batch, and our resulting models after a global merge consisted of 27-33 clusters. It is unreasonable to expect to find 10 clusters exactly due to the variation of handwritten digits within numbers. The increased number of clusters was not an artefact of the global merging; a run of MerDel on the MNIST test set of  $N = 10,000$  digits with 35 maximum clusters found between 33-35 clusters where most merges/deletes were rejected. Other unsupervised clustering models in the literature on MNIST datasets also found a high number of clusters (Hughes & Sudderth, 2013; Ni et al., 2020).

Figure S12 depicts the distribution of true number labels within each cluster, and demonstrates subclustering within digits in the ‘best’ model out of our 5 clustering structures. This is chosen as the model with the highest ELBO, an approach used in other variational models (Ueda & Ghahramani, 2002; Hughes & Sudderth, 2013). We expected imperfect performance due to the reduction of the image to a 1D vector; every pixel is treated as independent of one another, and we lose all information from the 2D images pertaining to correlation between nearby pixels. We found that, for example, 4, 7, 9 were often seen together in clusters; these numbers have quite similar shapes and have a variety of shapes (Figure S11). On the other hand, FedMerDel performed particularly well in distinguishing 0, 1, 2 and 6 from other digits; 95.95% of 1’s and 92.46% of 6’s were classified into clusters predominantly made up of that digit. Further classification rates can be found in Appendix K.2, as well as a comparison to other scalable clustering methods.

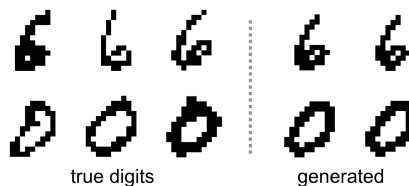


Figure 3. Three examples of digits assigned to Clusters 5 and 14 depicting 6’s and 0’s respectively, and two generated digits from the variational distribution of each cluster.

Furthermore, we can use the posterior distribution of our model to probabilistically produce new digits from each cluster, showing the generative potential in variational Bayes. An example of generated 0’s and 6’s is seen in Figure 3, and further examples can be seen in Appendix K.3.

Table 1. ‘Global Merge Simulations’ results. We report the median and lower/upper quantiles across all 10 ‘shuffles’/initialisations and all 10 synthetic datasets. FedMerDel results use random search; greedy search results are found in the Appendix, but differed little.

N	MODEL	BATCHES/CORES	ARI	CLUSTERS	TIME (s)
50000	FULL	5	0.947 [0.941, 0.954]	12 [12, 12]	467 [414, 554]
	PAR	5	0.948 [0.942, 0.954]	12 [12, 12]	176 [163, 196]
	FEDMERDEL	5	0.945 [0.939, 0.948]	12 [12, 12]	114 [106, 123]
100000	FULL	5	0.955 [0.944, 0.961]	12 [12, 12]	956 [861, 1116]
	PAR	5	0.954 [0.944, 0.961]	12 [12, 12]	338 [310, 380]
	FEDMERDEL	5	0.954 [0.943, 0.960]	12 [12, 12]	260 [232, 287]
200000	PAR	10	0.952 [0.947, 0.958]	12 [12, 12]	482 [446, 536]
	FEDMERDEL	10	0.951 [0.946, 0.957]	12.5 [12, 13]	270 [243, 305]
500000	PAR	10	0.950 [0.943, 0.951]	12 [12, 12]	1121 [1056, 1303]
	FEDMERDEL	10	0.949 [0.942, 0.951]	12.5 [12, 13]	688 [646, 797]

### 6.3. Electronic Health Record (EHR) data

We divided the data into 14 batches of size 20,000 and 1 batch of size 9,821, and ran FedMerDel with  $K = 20$  maximum clusters within each batch. After global merging, we obtained 8 clusters, which are summarised in Figure 4. Each cluster can be characterised by particular conditions. From top to bottom in Figure 4, we have clusters of individuals with: (i) cancer; (ii) Atrial fibrillation (AF) & arrhythmia; (iii) peripheral vascular disease & aortic aneurism; (iv) stroke; (v) AF & arrhythmia and stroke; (vi) blindness; (vii) dementia; and (viii) “generally multimorbid” individuals.

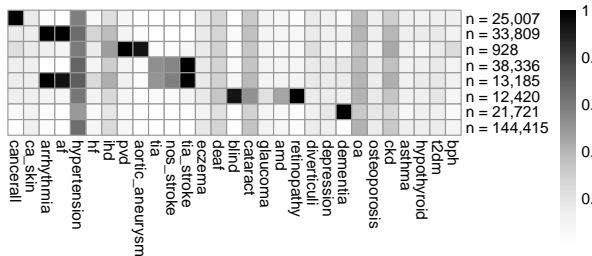


Figure 4. Results of EHR clustering. Columns are health conditions, and rows correspond to clusters. The shading indicates the proportion of individuals in each cluster that had each health condition, while row labels indicate the number of individuals in each cluster. To improve visualisation, only the most prevalent health conditions are shown (see Appendix L for further details and coding of health conditions).

## 7. Conclusion

In this manuscript, we introduced FedMerDel, a Bayesian mixture modelling algorithm using variational inference and ‘global’ merge moves to enable federated learning without sharing the full dataset across nodes. This model showed good performance on both simulated and real-world data, with only slight reductions in performance compared to

analysing the full dataset on one machine (when this is possible), and is particularly useful when federated learning is required.

The distribution of data into separate batches for initial inference before extending the merge move to a ‘global merge’, directly addressed both the challenge of scaling model-based clustering, and the challenge associated with clustering data which is decentralised and held in separate locations. This is important in scenarios where data privacy is a concern, such as with patient health records. We demonstrated that our method was effective in investigating multimorbidity in one anonymised EHR dataset. We showed that FedMerDel improved time efficiency compared to stepwise parallelisation of the usual variational EM algorithm, especially as dataset sizes increased. We further showed that variational distributions can be used to generate observations from a certain cluster.

There is clearly scope for improvement in some aspects of the model. For example, to scale up to even larger datasets, we could add extra steps in the global merge as in the SIGN model (Ni et al., 2019), where local clusters are combined over multiple steps over multiple computing cores.

While we presented our approach in the context of modelling large categorical datasets, we note that it can be straightforwardly adapted to mixtures of Gaussians and other members of the exponential family. The use of sufficient statistics to allow for efficient ELBO calculation in global merges could potentially extend to any exponential family distribution; (Hughes & Sudderth, 2013) provides some further details.

## Impact Statement

This paper presents work whose goal is to advance the field of Machine Learning. There are many potential societal consequences of our work, none which we feel must be specifically highlighted here.



## References

- Bishop, C. M. *Pattern Recognition and Machine Learning*. Information Science and Statistics. Springer, New York, NY, 1 edition, August 2006.
- Blei, D. M., Kucukelbir, A., and McAuliffe, J. D. Variational Inference: A Review for Statisticians. *Journal of the American Statistical Association*, 112(518):859–877, April 2017. ISSN 1537-274X. doi: 10.1080/01621459.2017.1285773.
- Boyd, S. and Vandenberghe, L. *Convex Optimization*. Cambridge University Press, 2004.
- Cao, L., Chen, H., Fan, X., Gama, J., Ong, Y.-S., and Kumar, V. Bayesian Federated Learning: A Survey. In Elkind, E. (ed.), *Proceedings of the Thirty-Second International Joint Conference on Artificial Intelligence, IJCAI-23*, pp. 7233–7242. International Joint Conferences on Artificial Intelligence Organization, 8 2023. doi: 10.24963/ijcai.2023/851. Survey Track.
- Celeux, G., Hurn, M., and Robert, C. P. Computational and Inferential Difficulties with Mixture Posterior Distributions. *Journal of the American Statistical Association*, 95(451):957–970, September 2000. ISSN 1537-274X. doi: 10.1080/01621459.2000.10474285.
- Chaturvedi, A., Green, P. E., and Carroll, J. D. K-modes Clustering. *Journal of Classification*, 18(1): 35–55, January 2001. ISSN 1432-1343. doi: 10.1007/s00357-001-0004-3.
- Dahl, D. B. and Newcomb, S. Sequentially allocated merge-split samplers for conjugate Bayesian nonparametric models. *Journal of Statistical Computation and Simulation*, 92(7):1487–1511, November 2021. ISSN 1563-5163. doi: 10.1080/00949655.2021.1998502.
- Diebolt, J. and Robert, C. P. Estimation of Finite Mixture Distributions through Bayesian Sampling. *Journal of the Royal Statistical Society. Series B (Methodological)*, 56(2):363–375, 1994. ISSN 00359246.
- Escobar, M. D. and West, M. Bayesian Density Estimation and Inference Using Mixtures. *Journal of the American Statistical Association*, 90(430):577–588, June 1995. ISSN 1537-274X. doi: 10.1080/01621459.1995.10476550.
- Ferguson, T. S. A Bayesian Analysis of Some Nonparametric Problems. *The Annals of Statistics*, 1(2), March 1973. ISSN 0090-5364. doi: 10.1214/aos/1176342360.
- Garst, S. and Reinders, M. Federated K-Means Clustering. In Antonacopoulos, A., Chaudhuri, S., Chellappa, R., Liu, C.-L., Bhattacharya, S., and Pal, U. (eds.), *Pattern Recognition*, pp. 107–122, Cham, 2025. Springer Nature Switzerland. ISBN 978-3-031-78166-7.
- Ghahramani, Z. and Beal, M. Propagation Algorithms for Variational Bayesian Learning. In Leen, T., Dietterich, T., and Tresp, V. (eds.), *Advances in Neural Information Processing Systems*, volume 13. MIT Press, 2000.
- Huang, Z. and Gelman, A. Sampling for Bayesian Computation with Large Datasets. *SSRN Electronic Journal*, 2005. ISSN 1556-5068. doi: 10.2139/ssrn.1010107.
- Hughes, M., Kim, D. I., and Sudderth, E. Reliable and Scalable Variational Inference for the Hierarchical Dirichlet Process. In Lebanon, G. and Vishwanathan, S. V. N. (eds.), *Proceedings of the Eighteenth International Conference on Artificial Intelligence and Statistics*, volume 38 of *Proceedings of Machine Learning Research*, pp. 370–378. PMLR, 09–12 May 2015.
- Hughes, M. C. and Sudderth, E. Memoized Online Variational Inference for Dirichlet Process Mixture Models. In *Advances in Neural Information Processing Systems*, volume 26. Curran Associates, Inc., 2013.
- Jain, S. and Neal, R. M. A Split-Merge Markov Chain Monte Carlo Procedure for the Dirichlet Process Mixture Model. *Journal of Computational and Graphical Statistics*, 13(1):158–182, 2004. ISSN 1061-8600.
- Kairouz, P., McMahan, H. B., Avent, B., Bellet, A., Bennis, M., Bhagoji, A. N., Bonawit, K., Charles, Z., Cormode, G., Cummings, R., D’Oliveira, R. G. L., Eichner, H., El Rouayheb, S., Evans, D., Gardner, J., Garrett, Z., Gascón, A., Ghazi, B., Gibbons, P. B., Gruteser, M., Harchaoui, Z., He, C., He, L., Huo, Z., Hutchinson, B., Hsu, J., Jaggi, M., Javidi, T., Joshi, G., Khodak, M., Konečný, J., Korolova, A., Koushanfar, F., Koyejo, S., Lepoint, T., Liu, Y., Mittal, P., Mohri, M., Nock, R., Özgür, A., Pagh, R., Qi, H., Ramage, D., Raskar, R., Raykova, M., Song, D., Song, W., Stich, S. U., Sun, Z., Theertha Suresh, A., Tramèr, F., Vepakomma, P., Wang, J., Xiong, L., Xu, Z., Yang, Q., Yu, F. X., Yu, H., and Zhao, S. *Advances and Open Problems in Federated Learning*. Now Foundations and Trends, 2021.
- Kuhn, H. W. The Hungarian method for the assignment problem. *Naval Research Logistics Quarterly*, 2(1-2):83–97, 1955. doi: <https://doi.org/10.1002/nav.3800020109>.
- Kumar, H. H., V R, K., and Nair, M. K. Federated K-Means Clustering: A Novel Edge AI Based Approach for Privacy Preservation. In *2020 IEEE International Conference on Cloud Computing in Emerging Markets (CCEM)*, pp. 52–56, 2020. doi: 10.1109/CCEM50674.2020.00021.

- Law, M., Figueiredo, M., and Jain, A. Simultaneous feature selection and clustering using mixture models. *IEEE Transactions on Pattern Analysis and Machine Intelligence*, 26(9):1154–1166, September 2004. ISSN 0162-8828. doi: 10.1109/tpami.2004.71.
- LeCun, Y., Cortes, C., and Burges, C. J. The MNIST Database. <https://yann.lecun.com/exdb/mnist/>, 2011. Accessed 2024-09-25.
- Leisch, F. FlexMix: A General Framework for Finite Mixture Models and Latent Class Regression in R. *Journal of Statistical Software*, 11(8), 2004. ISSN 1548-7660. doi: 10.18637/jss.v011.i08.
- Lin, D. Online Learning of Nonparametric Mixture Models via Sequential Variational Approximation. In Burges, C., Bottou, L., Welling, M., Ghahramani, Z., and Weinberger, K. (eds.), *Advances in Neural Information Processing Systems*, volume 26. Curran Associates, Inc., 2013.
- Liu, Y., Ma, Z., Yan, Z., Wang, Z., Liu, X., and Ma, J. Privacy-preserving federated k-means for proactive caching in next generation cellular networks. *Information Sciences*, 521:14–31, 2020. ISSN 0020-0255. doi: <https://doi.org/10.1016/j.ins.2020.02.042>.
- Maceachern, S. N. Estimating normal means with a conjugate style Dirichlet process prior. *Communications in Statistics - Simulation and Computation*, 23(3):727–741, January 1994. ISSN 1532-4141. doi: 10.1080/03610919408813196.
- Malsiner-Walli, G., Frühwirth-Schnatter, S., and Grün, B. Model-based clustering based on sparse finite Gaussian mixtures. *Statistics and Computing*, 26(1–2): 303–324, August 2014. ISSN 1573-1375. doi: 10.1007/s11222-014-9500-2.
- Mansinghka, V., Shafto, P., Jonas, E., Petschulat, C., Gasner, M., and Tenenbaum, J. B. CrossCat: A Fully Bayesian Nonparametric Method for Analyzing Heterogeneous, High Dimensional Data. *Journal of Machine Learning Research*, 17(138):1–49, 2016.
- McMahan, B., Moore, E., Ramage, D., Hampson, S., and Arcas, B. A. y. Communication-Efficient Learning of Deep Networks from Decentralized Data. In Singh, A. and Zhu, J. (eds.), *Proceedings of the 20th International Conference on Artificial Intelligence and Statistics*, volume 54 of *Proceedings of Machine Learning Research*, pp. 1273–1282. PMLR, 20–22 Apr 2017.
- Nallapati, R., Cohen, W., and Lafferty, J. Parallelized Variational EM for Latent Dirichlet Allocation: An Experimental Evaluation of Speed and Scalability. In *Seventh IEEE International Conference on Data Mining Workshops (ICDMW 2007)*, pp. 349–354. IEEE, October 2007. doi: 10.1109/icdmw.2007.33.
- Neal, R. M. Markov Chain Sampling Methods for Dirichlet Process Mixture Models. *Journal of Computational and Graphical Statistics*, 9(2):249–265, 2000. ISSN 10618600.
- Neal, R. M. and Hinton, G. E. *A View of the EM Algorithm that Justifies Incremental, Sparse, and other Variants*, pp. 355–368. Springer Netherlands, Dordrecht, 1998. ISBN 978-94-011-5014-9. doi: 10.1007/978-94-011-5014-9\_12.
- Neiswanger, W., Wang, C., and Xing, E. Embarrassingly Parallel Variational Inference in Nonconjugate Models. *arXiv preprint arXiv:1510.04163*, 2015.
- Ni, Y., Müller, P., Diesendruck, M., Williamson, S., Zhu, Y., and Ji, Y. Scalable Bayesian Nonparametric Clustering and Classification. *Journal of Computational and Graphical Statistics*, 29(1):53–65, July 2019. ISSN 1537-2715. doi: 10.1080/10618600.2019.1624366.
- Ni, Y., Ji, Y., and Müller, P. Consensus Monte Carlo for Random Subsets Using Shared Anchors. *Journal of Computational and Graphical Statistics*, 29(4):703–714, April 2020. ISSN 1537-2715. doi: 10.1080/10618600.2020.1737085.
- Rabinovich, M., Angelino, E., and Jordan, M. I. Variational Consensus Monte Carlo. In Cortes, C., Lawrence, N., Lee, D., Sugiyama, M., and Garnett, R. (eds.), *Advances in Neural Information Processing Systems*, volume 28. Curran Associates, Inc., 2015.
- Rao, J. and Kirk, P. D. W. VICatMix: variational Bayesian clustering and variable selection for discrete biomedical data. *arXiv preprint arXiv:2406.16227*, 2024. doi: 10.48550/ARXIV.2406.16227.
- Richardson, S. and Green, P. J. On Bayesian Analysis of Mixtures with an Unknown Number of Components (with discussion). *Journal of the Royal Statistical Society: Series B (Statistical Methodology)*, 59(4):731–792, 1997. doi: <https://doi.org/10.1111/1467-9868.00095>.
- Robert, C. P. and Casella, G. *Monte Carlo Statistical Methods*. Springer New York, 2004. ISBN 9781475741452. doi: 10.1007/978-1-4757-4145-2.
- Rousseau, J. and Mengersen, K. Asymptotic Behaviour of the Posterior Distribution in Overfitted Mixture Models. *Journal of the Royal Statistical Society Series B: Statistical Methodology*, 73(5):689–710, August 2011. ISSN 1467-9868. doi: 10.1111/j.1467-9868.2011.00781.x.

- Savage, R. S., Ghahramani, Z., Griffin, J. E., Kirk, P. D. W., and Wild, D. L. Identifying cancer subtypes in glioblastoma by combining genomic, transcriptomic and epigenomic data. *arXiv preprint arXiv:1304.3577*, 2013.
- Scott, S. L., Blocker, A. W., Bonassi, F. V., Chipman, H. A., George, E. I., and McCulloch, R. E. Bayes and big data: the consensus Monte Carlo algorithm. *International Journal of Management Science and Engineering Management*, 11(2):78–88, February 2016. ISSN 1750-9661. doi: 10.1080/17509653.2016.1142191.
- Tadesse, M. G., Sha, N., and Vannucci, M. Bayesian Variable Selection in Clustering High-Dimensional Data. *Journal of the American Statistical Association*, 100(470):602–617, June 2005. ISSN 1537-274X. doi: 10.1198/016214504000001565.
- Tian, Y., Weng, H., and Feng, Y. Towards the Theory of Unsupervised Federated Learning: Non-asymptotic Analysis of Federated EM algorithms. In *Forty-first International Conference on Machine Learning*, 2024.
- Ueda, N. and Ghahramani, Z. Bayesian model search for mixture models based on optimizing variational bounds. *Neural Networks*, 15(10):1223–1241, December 2002. ISSN 0893-6080. doi: 10.1016/s0893-6080(02)00040-0.
- Ueda, N., Nakano, R., Ghahramani, Z., and Hinton, G. E. SMEM Algorithm for Mixture Models. *Neural Computation*, 12(9):2109–2128, September 2000. ISSN 0899-7667, 1530-888X. doi: 10.1162/089976600300015088.
- van Havre, Z., White, N., Rousseau, J., and Mengersen, K. Overfitting Bayesian Mixture Models with an Unknown Number of Components. *PLOS ONE*, 10(7):e0131739, July 2015. ISSN 1932-6203. doi: 10.1371/journal.pone.0131739.
- Walker, S. G. Sampling the Dirichlet Mixture Model with Slices. *Communications in Statistics - Simulation and Computation*, 36(1):45–54, January 2007. ISSN 1532-4141. doi: 10.1080/03610910601096262.
- Yang, Y., Chen, B., and Liu, H. Memorized Variational Continual Learning for Dirichlet Process Mixtures. *IEEE Access*, 7:150851–150862, 2019. ISSN 2169-3536. doi: 10.1109/access.2019.2947722.
- Zhu, J., Chen, J., Hu, W., and Zhang, B. Big Learning with Bayesian methods. *National Science Review*, 4(4): 627–651, 05 2017. ISSN 2095-5138. doi: 10.1093/nsr/nwx044.
- Zuanetti, D. A., Müller, P., Zhu, Y., Yang, S., and Ji, Y. Bayesian nonparametric clustering for large data sets. *Statistics and Computing*, 29(2):203–215, February 2018. ISSN 1573-1375. doi: 10.1007/s11222-018-9803-9.

## Appendix

### A. Variable Selection

As explored in Law et al. (2004) and Tadesse et al. (2005), we can introduce binary feature selection indicators  $\gamma_j$  - feature saliencies - where  $\gamma_j = 1$  if and only if the  $j$ -th covariate is relevant to the clustering structure, and irrelevant variables have their feature saliencies reduced to zero. The probability density for a data point  $x_n$  in cluster  $k$  is given by:

$$f(\mathbf{x}_n | \Phi_k) = \prod_{j=1}^P f_j(x_{nj} | \Phi_{kj})^{\gamma_j} f_j(x_{nj} | \Phi_{0j})^{1-\gamma_j} \quad (16)$$

$\Phi_{0j} = [\phi_{0j1}, \dots, \phi_{0jL_j}]$  are parameter estimates obtained for covariate  $j$  under the assumption that there exists no clustering structure in the  $j$ -th covariate. These are precomputed using maximum likelihood estimates as seen in Savage et al. (2013). The priors associated with  $\gamma_j$  for  $j = 1, \dots, P$  are as follows:

$$\gamma_j | \delta_j \sim \text{Bernoulli}(\delta_j) \quad (17)$$

$$\delta_j \sim \text{Beta}(a, a) \quad (18)$$

### B. Hyperparameters

We detail here further parameter settings for the priors detailed in Section 2.1 of the main paper.

- $\phi$ :  $\epsilon_{jl} = 1/L_j$  for each  $j = 1, \dots, P, l = 1, \dots, L_j$ . There is no prior favouring for a variable to take a certain value in any of the clusters.
- $\gamma, \delta$ : We set the hyperparameter for  $\delta$  to be  $a = 2$  in all simulations, as in Rao & Kirk (2024). The use of a hyperprior for  $\gamma$  allows the prior probability of the inclusion of each covariate to be a target for inference. In the variational algorithm, initially we include all variables by setting  $c_j = \mathbb{E}_\gamma(\gamma_j) = 1$  for all  $j = 1, \dots, P$ . Variables are found to be irrelevant as the algorithm runs.

### C. Mean-Field Variational Inference (VI)

To improve the readability and continuity of the supplementary material, some content from the main manuscript is repeated in this section. The true Bayesian posterior distribution is intractable as it is computationally intractable to evaluate the marginal likelihood  $p(X)$ . We employ a variational inference (VI) approach to seek an approximate distribution  $q$  which is as close as possible to the true posterior. We do this by optimising the Evidence Lower Bound (ELBO) given below,  $\mathcal{L}(q)$ , with respect to  $q(\theta)$ , where  $\theta$  is a collection of all parameters in the model.

$$\mathcal{L}(q) = \int q(\theta) \ln \left( \frac{p(X, \theta)}{q(\theta)} \right) d\theta \quad (19)$$

This is equivalent to minimising the Kullback-Leibler (KL) divergence between  $q(\theta)$  and the true posterior,  $p(\theta|X)$ . We constrain  $q$  to be a mean-field approximation which can be fully factorised as (in the variable selection setting):  $q(\theta) = q_Z(Z)q_\pi(\pi)q_\Phi(\Phi)q_\gamma(\gamma)q_\delta(\delta)$ . The mean-field approximation is simple enough for tractable approximation of the ELBO, and is sufficiently flexible to provide good approximations.

In mean-field VI, the optimal solution  $q_j^*(\theta_j)$  for each component of  $\theta, \theta_j$ , satisfies (Bishop, 2006):

$$q_j^*(\theta_j) = \frac{\exp(\mathbb{E}_{i \neq j}[\ln p(X, \theta)])}{\int \exp(\mathbb{E}_{i \neq j}[\ln p(X, \theta)]) d\theta_j} \quad (20)$$

We adopt an iterative procedure to optimise  $\mathcal{L}(q)$  by cycling between optimising  $q(\theta)$  with respect to each parameter in turn. This numerical procedure is analogous to an Expectation-Minimisation (EM) algorithm, and the variational Bayes algorithm can be reduced to the EM algorithm by setting the variational densities to point estimates (Neal & Hinton, 1998;

Ghahramani & Beal, 2000). As the ELBO is convex with respect to each factor  $q_j^*(\theta_j)$ , convergence of the algorithm is guaranteed (Boyd & Vandenberghe, 2004). The ELBO is calculated after every EM step, and we can use sufficient statistics (similar to those detailed in Section 4.2) to reduce computation in sums over  $N$  in the ELBO. This improves the efficiency of the overall algorithm. It is important to note that the frequency of ELBO calculations is a factor contributing to the overall run-time of any variational algorithm.

**‘E’ Step** In the variational ‘E’ (expectation) step, the latent variables  $Z$  are updated using the current variational distributions of all other parameters ( $q^*(\pi)$ ,  $q^*(\phi)$  and  $q^*(\gamma)$ ,  $q^*(\delta)$  in the variable selection case). Using Equation 20, in the model without variable selection, we have:

$$q^*(Z) = \prod_{n=1}^N \prod_{k=1}^K r_{nk}^{z_{nk}}, \quad r_{nk} = \frac{\rho_{nk}}{\sum_{j=1}^K \rho_{nj}} \quad (21)$$

$$\ln \rho_{nk} = \mathbb{E}_\pi[\ln \pi_k] + \sum_{i=1}^P \mathbb{E}_\Phi[\ln \phi_{kix_{ni}}] \quad (22)$$

$r_{nk}$  is the responsibility of the  $k$ -th component for the  $n$ -th observation, and  $\mathbb{E}[z_{nk}] = r_{nk}$ . Data point  $n$  is allocated to cluster  $k^*$  where  $k^* = \arg \max_k r_{nk}$ .

**‘M’ Step** Given updated responsibilities  $r_{nk}$  in the ‘E’ step, the variational ‘M’ (maximisation) step updates cluster-specific parameters (and variable selection parameters) in the model.

$$q^*(\pi) = \text{Dirichlet}(\alpha_1^*, \dots, \alpha_K^*) \quad (23)$$

$$q^*(\phi) = \prod_{k=1}^K \prod_{j=1}^P \text{Dirichlet}(\epsilon_{kj1}^*, \dots, \epsilon_{kjL_j}^*) \quad (24)$$

where for  $k = 1, \dots, K, j = 1, \dots, P, l = 1, \dots, L_j$ :

$$\alpha_k^* = \alpha_0 + \sum_{n=1}^N r_{nk} \quad (25)$$

$$\epsilon_{kjl}^* = \epsilon_j + \sum_{n=1}^N \mathbb{I}(x_{nj} = l) r_{nk} \quad (26)$$

Expectations throughout are taken with respect to variational distributions. Between each ‘E’ and ‘M’ step, we calculate the value of the ELBO and use this to monitor convergence. All values are initialised using k-modes (Chaturvedi et al., 2001), a method analogous to k-means for categorical data.

## D. Variational Updates with Variable Selection

**‘E’ Step** This follows a similar form to the model with no variable selection, where  $Z$  takes a multinomial distribution.

$$q^*(Z) = \prod_{n=1}^N \prod_{k=1}^K r_{nk}^{z_{nk}}, \quad r_{nk} = \frac{\rho_{nk}}{\sum_{j=1}^K \rho_{nj}} \quad (27)$$

$$\ln \rho_{nk} = \mathbb{E}_\pi[\ln \pi_k] + \sum_{j=1}^P c_j \mathbb{E}_\Phi[\ln \phi_{kjx_{nj}}] + (1 - c_j)(\ln \phi_{0jx_{nj}}) \quad (28)$$

$c_j = \mathbb{E}_\gamma(\gamma_j)$ , where the expectation is taken over the variational distribution for  $\gamma$ .

**‘M’ Step** Similarly to the model with no variable selection, the updates for the cluster-specific parameters are given by:

$$q^*(\pi) = \text{Dirichlet}(\alpha_1^*, \dots, \alpha_K^*) \quad (29)$$

$$q^*(\phi) = \prod_{k=1}^K \prod_{j=1}^P \text{Dirichlet}(\epsilon_{kj1}^*, \dots, \epsilon_{kjL_j}^*) \quad (30)$$

where for  $k = 1, \dots, K, j = 1, \dots, P, l = 1, \dots, L_j$ :

$$\alpha_k^* = \alpha_k + \sum_{n=1}^N r_{nk}, \quad \epsilon_{kjl}^* = \epsilon_j + \sum_{n=1}^N \mathbb{I}(x_{nj} = l) r_{nk} c_j \quad (31)$$

The updates for  $\gamma$  and  $\delta$  are given as:

$$q^*(\gamma_j) = \text{Bernoulli}(c_j), \quad c_j = \frac{\eta_{1j}}{\eta_{1j} + \eta_{2j}} = \mathbb{E}_\gamma(\gamma_j) \quad (32)$$

$$\ln \eta_{1i} = \sum_{n=1}^N \sum_{k=1}^K (r_{nk} \mathbb{E}_\Phi[\ln \phi_{kjx_{nj}}]) + \mathbb{E}_\delta[\ln \delta_j] \quad (33)$$

$$\ln \eta_{2i} = \sum_{n=1}^N \sum_{k=1}^K (r_{nk} \ln \phi_{0jx_{nj}}) + \mathbb{E}_\delta[\ln(1 - \delta_j)] \quad (34)$$

$$q^*(\delta_j) = \text{Beta}(c_j + a, 1 - c_j + a) \quad (35)$$

All expectations throughout are taken over the variational distributions for each parameter. The general algorithm involves cycling between performing the ‘E’ step to evaluate the values of  $r_{nk}$  with the current parameter values, and then the ‘M’ step to re-optimize all cluster-specific parameters and variable selection parameters.

## E. Merge and Delete Moves: Further Detail

### E.1. Merge Moves

Merge moves refer to moves that combine observations from two clusters into one unified cluster. Suppose clusters  $k_1$  and  $k_2$  are considered for a merge. We propose a move to reassign all observations from clusters  $k_1$  and  $k_2$  into a single new cluster,  $k^*$ . The responsibilities for this new cluster are given by  $r_{nk^*} = r_{nk_1} + r_{nk_2}$ . All other responsibilities for other clusters remain the same.

We then perform a ‘dummy’ variational M step, updating the  $\pi, \phi$  parameters. We run an extra E and an extra M step to allow observations to move in or out of the new cluster. We then calculate the ELBO and compare this to the ELBO before the merge move; we accept this move if the ELBO has improved, otherwise we return to the model prior to the merge. If accepted, we reassign cluster  $k^*$  to the  $k_1$  position and delete cluster  $k_2$  from the model.

#### E.1.1. SELECTING CANDIDATE CLUSTERS TO MERGE

We could choose a pair of clusters for a merge at random, but a merge is more likely to be accepted if the two clusters are ‘similar’. Making informed decisions on which pair of clusters to propose for a merge can improve efficiency by reducing the number of rejected merge moves. Two methods of assessing similarity between clusters using correlation and divergences between variational distributions are detailed below. Other ways include comparing marginal likelihoods or posterior probabilities of candidate models as in [Hughes et al. \(2015\)](#) and [Ueda et al. \(2000\)](#).

Due to the stochastic nature of the selection from the ‘candidate clusters’, similar results between different merge candidates are to be expected and the choice of measure is insignificant. Results from a simulation study comparing selection criteria for clusters to be merged are seen in [Appendix J.4](#). Correlation and divergence-based methods performed similarly, but did provide a reduction in overall computation time and an improvement in rates of accepted merges compared to random selection.

**Correlation** We can use an assessment of correlation between the variational parameters associated with each cluster. For example, in [Hughes & Sudderth \(2013\)](#), two topics in the hierarchical Dirichlet process are proposed for a merge if the correlation between statistics representing usage of the topic across documents is above 0.05.

We can construct a correlation score by looking at the correlation between the parameter values  $\epsilon^*$  in the distributions  $q(\phi_{k,j})$ . In the binary case, each  $\epsilon_{k,j}^*$  is given by a two dimensional vector, and without loss of generality, for each  $k$ , we can take the first value of each of these vectors for  $j = 1, \dots, P$ , concatenate these into one  $j$  length vector,  $\epsilon_k^{corr}$  and then compare the correlation of these concatenated vectors across clusters. The  $\epsilon_k^{corr}$  values represent the (expected) frequency of 0's in each cluster across all variables in a binary dataset of 0's and 1's.

We select randomly between the 3 cluster pairs with the highest correlation, provided  $\text{Corr}(\epsilon_{k_1}^{corr}, \epsilon_{k_2}^{corr})$  is above 0.05. With the categorical case with  $L$  categories per variable, we could consider finding the correlation scores for  $L - 1$  concatenated vectors across all variables for  $L - 1$  of the categories (avoiding overparameterisation) and taking the mean correlation score for comparison. However, this is complicated when variables have different numbers of categories, and this method is less straightforward to extend to other probability distributions.

**Divergence-based Measures** We also look at using measures of distance between probability distributions to quantify similarity between clusters. For a pair of clusters  $k_1$  and  $k_2$ , we look at the divergence between  $q(\phi_{k_1,j})$  and  $q(\phi_{k_2,j})$  and sum over all variables  $j$  for a pair of clusters  $k_1$  and  $k_2$ . We then choose randomly between the 3 cluster pairs with the lowest divergences, for example.

Different divergences could be considered; in this paper we considered both the Kullback-Leibler (KL) divergence and the Bhattacharyya distance. We emphasise that we are not seeking an exact, precise characterisation of the 'distance' but are only making approximate comparisons between candidate cluster pairs.

## E.2. Delete Moves

Delete moves refer to moves to delete unnecessary extra clusters in the model. Redundant small clusters often remain at local optima in variational algorithms for mixture models. These clusters are usually inconsistent across different initialisations, suggesting that moves to remove them and reassign observations to other clusters could improve performance.

Let cluster  $k$  be a candidate cluster for deletion. For the set of observations in cluster  $k$ , ie.  $S_k := \{n = 1 \dots N : z_{nk} = 1\}$ , we create a new data-frame  $X_{-k}$  with the rows from observations in  $S_k$  removed, and the column for cluster  $k$  removed. We first perform the variational E step after removing all variational parameters relevant to cluster  $k$  in the model. This recalculates all responsibilities for the remaining observations. We then perform the variational M step, which updates the  $\pi, \phi$  (and  $\gamma, \delta$  if variable selection is used) parameters.

We then return to the original dataframe  $X$  and then run an E step using  $X$  with the current model parameters, which reassigns all observations in  $X$  to new clusters. After performing another M step, we then calculate the value of the ELBO function. We accept the delete move if the new ELBO is higher.

Note that in both the merge and delete moves described above, there is an extremely small approximation involved in setting  $r_{nk} = 0$  exactly for responsibilities associated with clusters 'removed' in merge/delete moves. We go into further detail in [Appendix H](#), showing that this approximation simply replaces numbers extremely close to 0 (numbers smaller than  $10^{-80}$ ) during the algorithm and has virtually no effect on the clustering structure.

### E.2.1. SELECTING CANDIDATE CLUSTERS TO DELETE

Smaller clusters are likely to be better candidates for deletion as it is likely these observations have been 'left out'. Extremely small clusters are also less informative in practical applications and may be less reproducible in other similar independent datasets. In this paper, we propose a cluster chosen randomly between all clusters which are smaller than 5% of the dataset; if there are none, we choose randomly between the three smallest clusters. As in [Appendix E.1.1](#), the stochasticity of this process means that other methods should not give significantly different results.

## F. Global ELBO Calculation - Further Details

For the model with no variable selection, the ELBO for the full dataset is given by:

$$\begin{aligned}\mathcal{L}(q) &= \mathbb{E}_{Z,\pi,\Phi}[\ln p(X, Z, \pi, \Phi)] - \mathbb{E}_{Z,\pi,\Phi}[\ln q(Z, \pi, \Phi)] \\ &= \mathbb{E}_{Z,\Phi}[\ln p(X|Z, \Phi)] + \mathbb{E}_{Z,\pi}[\ln p(Z|\pi)] + \mathbb{E}_\pi[\ln p(\pi)] + \mathbb{E}_\Phi[\ln p(\Phi)] \\ &\quad - \mathbb{E}_Z[\ln q(Z)] - \mathbb{E}_\pi[\ln q(\pi)] - \mathbb{E}_\Phi[\ln q(\Phi)]\end{aligned}\quad (36)$$

where all expectations are taken with respect to the variational distributions for  $Z, \pi, \Phi$ . From standard properties of the Dirichlet distribution, we initially calculate:

$$\mathbb{E}_\pi[\ln \pi_k] = \psi(\alpha_k^*) - \psi\left(\sum_{k=1}^K \alpha_k^*\right) \quad (37)$$

$$\mathbb{E}_\Phi[\ln \phi_{kjl}] = \psi(\epsilon_{kjl}^*) - \psi\left(\sum_{l=1}^{L_j} \epsilon_{kjl}^*\right) \quad (38)$$

where  $\psi(x)$  refers to the digamma function.

As written in the main text of the paper, we also use the current  $\alpha^*$  and  $\epsilon^*$  values to calculate the values of sufficient statistics:

$$T_k = \sum_{n=1}^N r_{nk} = \alpha_k^* - \alpha_0 \quad (39)$$

$$S_{kjl} = \sum_{n=1}^N r_{nk} \mathbb{I}(x_{nj} = l) = \epsilon_{kjl}^* - \epsilon_{jl} \quad (40)$$

Each term in Equation (37) is as follows:

$$\mathbb{E}_{Z,\Phi}[\ln p(X|Z, \Phi)] = \mathbb{E}_{Z,\Phi}\left[\sum_{n=1}^N \sum_{k=1}^K z_{nk} \left(\sum_{j=1}^P \ln \phi_{kjx_{nj}}\right)\right] \quad (41)$$

$$= \sum_{n=1}^N \sum_{k=1}^K r_{nk} \left(\sum_{j=1}^P \mathbb{E}_\Phi[\ln \phi_{kjx_{nj}}]\right) \quad (42)$$

$$= \sum_{n=1}^N \sum_{k=1}^K \sum_{j=1}^P \sum_{l=1}^{L_j} r_{nk} \mathbb{I}(x_{nj} = l) \mathbb{E}_\Phi[\ln \phi_{kjl}] \quad (43)$$

$$= \sum_{k=1}^K \sum_{j=1}^P \sum_{l=1}^{L_j} S_{kjl} \mathbb{E}_\Phi[\ln \phi_{kjl}] \quad (44)$$

$$\mathbb{E}_{Z,\pi}[\ln p(Z|\pi)] = \mathbb{E}_{Z,\pi}\left[\sum_{n=1}^N \sum_{k=1}^K z_{nk} \ln \pi_k\right] \quad (45)$$

$$= \sum_{n=1}^N \sum_{k=1}^K r_{nk} \mathbb{E}_\pi[\ln \pi_k] \quad (46)$$

$$= \sum_{k=1}^K T_k \mathbb{E}_\pi[\ln \pi_k] \quad (47)$$



$$\mathbb{E}_\pi[\ln p(\pi)] = -\ln B(\alpha) + \sum_{k=1}^K (\alpha_k - 1) \mathbb{E}_\pi[\ln \pi_k] \quad (48)$$

$$\mathbb{E}_\Phi[\ln p(\Phi)] = \sum_{k=1}^K \sum_{j=1}^P (-\ln B(\epsilon_{kj})) + \sum_{l=1}^{L_j} (\epsilon_{kjl} - 1) \mathbb{E}_\Phi[\ln \phi_{kjl}] \quad (49)$$

$$\mathbb{E}_Z[\ln q(Z)] = \sum_{n=1}^N \sum_{k=1}^K r_{nk} \ln r_{nk} \quad (\text{assignment entropy}) \quad (50)$$

$$\mathbb{E}_\pi[\ln q(\pi)] = -\ln B(\alpha^*) + \sum_{k=1}^K (\alpha_k^* - 1) \mathbb{E}_\pi[\ln \pi_k] \quad (51)$$

$$\mathbb{E}_\Phi[\ln q(\Phi)] = \sum_{k=1}^K \sum_{j=1}^P (-\ln B(\epsilon_{kj}^*)) + \sum_{l=1}^{L_j} (\epsilon_{kjl}^* - 1) \mathbb{E}_\Phi[\ln \phi_{kjl}] \quad (52)$$

Apart from the assignment entropy term in Equation (50), as we have calculated  $T_k$  and  $S_{kjl}$  via simple linear operations on our model parameters, there are no sums over  $N$  and all terms are mainly sums over much smaller  $K, P, L_j$ . Furthermore, there are terms in  $B(\alpha), B(\alpha^*), B(\epsilon_{kj}), B(\epsilon_{kj}^*)$  which cancel out - see Appendix H for more details. Importantly,  $X$  appears nowhere in the calculations; our global merge move allows us to seek a global clustering structure without any full scan over the  $N \times P$  matrix  $X$ .

For the assignment entropy term  $\sum_{n=1}^N \sum_{k=1}^K r_{nk} \ln r_{nk}$ , as detailed in the main paper, we can either calculate this value in parallel across different batches of observations across different cores, or in the case of the greedy search, this value remains constant as the merge moves only allow merges between clusters from different batches.

## G. Global Merge - Variable Selection

When finding a global clustering structure in the model with variable selection, our focus is on updating cluster allocation via merging local clusters, so we use the same global ELBO function as in the model without variable selection and only update  $Z, \pi, \phi$ . The nature of  $\phi$  updates in the model with variable selection means that the  $\epsilon^*$  parameters are equal to the prior parameters for the given covariate if a covariate is irrelevant in the model, so variable selection is still involved with the usual global merge move. Implementing this amounts to a small approximation in the true ELBO for the true Bayesian model.

We consider a variable to be ‘selected’ based on the percentage of times a variable was selected across the batches. In later simulations, we consider a variable selected if it was selected in either all batches, or all but one batch. This borrows ideas of ‘thresholds’ for variable selection across multiple VI runs which is seen in Rao & Kirk (2024).

## H. Approximations and Priors in MerDel

In Appendix E, we detailed that in the process of performing our merge/delete moves, we ‘remove’ the clusters by removing all parameters and responsibilities associated with this cluster in the model code. This could raise concerns pertaining to transdimensional inference, as on the surface, we are deleting a dimension of our model and the variational posterior now has a different dimension.

However, we still implicitly account for the removed clusters in subsequent calculations. We call these removed clusters ‘zombie clusters’; despite not technically remaining in the model in the code, they are never truly removed but instead ruled only by priors. This is because the cluster-specific parameters  $\alpha, \epsilon$  are determined by the prior only (as there is no data assigned to the cluster to update the cluster-specific parameters - see Section H.1). We can take these ‘zombie clusters’ into account in subsequent iterations of the algorithm and accurately calculate eg. ELBO values at each variational EM step by tracking the number of ‘zombie clusters’ we have.

There is an approximation made where we set responsibilities associated with ‘zombie clusters’ to 0 (by removing the responsibilities associated with the cluster). These responsibilities are not usually exactly 0. However, we describe below

how the responsibilities removed are infinitesimally small for the empty cluster  $k$  for all  $n$  and no observations are assigned to the cluster.

### H.1. Emptying a Cluster + M Update

In both the merge and delete settings, when a cluster  $k^*$  is removed, this is equivalent to assigning  $r_{nk^*} = 0$  for all observations  $n$ , as  $r_{nk^*}$  only appears in future calculations within sums. Therefore, we can think of our  $N \times K_{\text{init}}$  responsibility matrix as now having values of 0 in column  $k^*$ . After that, in both moves, we then perform a variational M step, where cluster-specific parameters  $\alpha^*$ ,  $\epsilon^*$  are updated:

$$\alpha_k^* = \alpha_0 + \sum_{n=1}^N r_{nk}, \quad \epsilon_{kjl}^* = \epsilon_{jl} + \sum_{n=1}^N \mathbb{I}(x_{nj} = l) r_{nk} \quad (53)$$

As we have that  $r_{nk} = 0$  for all  $n = 1, \dots, N$  for a removed cluster  $k$ ,  $\alpha_k^* = \alpha_0$  and  $\epsilon_{kjl}^* = \epsilon_{jl}$ . These variational posteriors for cluster  $k$  are solely ruled by the priors for  $\pi$  and  $\Phi$ .

### H.2. The Approximation: E Update

In MerDel, we then perform a variational E update with the full dataset (and another variational M update) to allow observations to move between clusters after the cluster-specific parameter updates. Recall that responsibilities  $r_{nk}$  are defined by:

$$r_{nk} = \frac{\rho_{nk}}{\sum_{j=1}^K \rho_{nj}}, \quad \ln \rho_{nk} = \mathbb{E}_\pi[\ln \pi_k] + \sum_{j=1}^P \mathbb{E}_\Phi[\ln \phi_{kjx_{nj}}] \quad (54)$$

The expectations in  $\ln \rho_{nk}$  are given by:

$$\mathbb{E}_\pi[\ln \pi_k] = \psi(\alpha_k^*) - \psi\left(\sum_{k=1}^K \alpha_k^*\right) \quad (55)$$

$$\mathbb{E}_\Phi[\ln \phi_{kjx_{nj}}] = \psi(\epsilon_{kjx_{nj}}^*) - \psi\left(\sum_{l=1}^{L_j} \epsilon_{kjl}^*\right) \quad (56)$$

For  $x > 0$ , the digamma function  $\psi(x)$  increases approximately in an exponential fashion.

For every cluster with observations assigned to it, we generally see that the observations are assigned to it with responsibilities close to 1. Looking at Equation (53), we see that  $\alpha_k^*$  is often a high value approximately on the scale of the number of observations assigned to the cluster - sometimes in the thousands for our dataset sizes - and the value of  $\alpha_0$ , which is chosen to be smaller than 1, has a very small impact.  $\alpha_k^*$  must be larger for any cluster with observations compared to any ‘zombie cluster’ as  $\alpha_k^*$  is a sum of non-negative responsibilities added to  $\alpha_0$ .  $\epsilon^*$  values are similar. Therefore, from Equations (55) and (56),  $\ln \rho_{nk}$  is much smaller for ‘zombie clusters’.  $\rho_{nk}$  is exponentially small in comparison to other cluster, and we find that after the normalising these values,  $r_{nk}$  values are *extremely* close to 0.

It is also almost impossible that these  $r_{nk}$  values will ever become larger as we continue through the EM steps;  $\alpha^*$  and  $\epsilon^*$  still remain extremely small for removed clusters (virtually equal to the values of the prior) in comparison to clusters with observations, and  $r_{nk}$  values still remain virtually 0, and the cycle continues. Our approximation is equivalent to setting these  $r_{nk}$  values to 0 permanently by removing these columns, allowing for computational efficiency and lower memory usage. We also do not perform inference for any further cluster-specific parameters associated with cluster  $k$  (by removing these values too) as they are always the same as their prior values if we set  $r_{nk} = 0$ . This saves wasted computation on these values. This approximation has virtually no effect on our model; we run two small simulations comparing the effects of implementing this approximation, and saw that true  $r_{nk}$  values were often on the scale of  $10^{-70}$  to  $10^{-100}$  on typical MerDel example datasets (see Section H.2.1).

We then go through and perform another M step as in the previous section, before evaluating the ELBO as detailed in the next section. Going forward with the algorithm after an accepted MerDel proposal, the variational E and M steps and

ELBO calculations continue as in this appendix, where  $r_{nk}$  values are set to be exactly 0 forever, and we remove all values associated with removed clusters.

This is in line with what we see in the overfitted variational model without merge/delete; when clusters are ‘emptied’, they are usually never filled again with observations. When there are no observations assigned to a cluster,  $\alpha^*$  and  $\epsilon^*$  values are given by their prior values, and we see that  $\ln \rho_{nk}$  is again much smaller for a cluster with no observations assigned to it compared to clusters with observations, and  $r_{nk}$  is close to 0. Under the overfitted model, it is virtually impossible that these clusters are ever filled again, and  $r_{nk}$  values will remain extremely close to 0 as illustrated above.

### H.2.1. SIMULATION IN MORE DETAIL

We set up 10 simulated datasets, and compared two versions of MerDel. We performed 5 runs of the ‘fast’ version of MerDel (removing columns associated with zombie clusters) and 5 runs of the ‘slow’ version of MerDel (not removing columns associated with zombie clusters) on each simulated dataset. We used the same initialisations for the ‘fast’ and ‘slow’ versions (by setting the same random number seed). For our first simulation, each dataset had  $N = 2000$ ,  $P = 100$ , 10 true clusters and was initialised with 15 maximum clusters, laps = 5 and  $\alpha_0 = 0.01$ . For the second simulation, each dataset had  $N = 10000$ ,  $P = 100$ , 10 true clusters and was initialised with 15 maximum clusters, laps = 1 and  $\alpha_0 = 0.01$ .

We measured the RMSE between the final  $r_{nk}$  matrices (inserting 0’s for ‘missing’ columns in the ‘fast’ MerDel version) and ARI between the final cluster labels. In both simulations, all ARIs between corresponding ‘fast’ and ‘slow’ clustering structures were 1 (perfect similarity). In the first simulation, the RMSE between  $r_{nk}$  matrices ranged between  $7.15 \times 10^{-84}$  and  $4.32 \times 10^{-80}$  (with a mean of  $6.63 \times 10^{-81}$ ); in the second simulation, the RMSE ranged between  $2.85 \times 10^{-83}$  and  $2.20 \times 10^{-80}$  (with a mean of  $2.78 \times 10^{-81}$ ). When only considering  $r_{nk}$  values for non-empty clusters, the RMSE was 0. The time taken for the ‘slow’ runs was indeed slower; for example, in the second simulation, the ‘fast’ runs took a mean time of 88.2 seconds to converge, while the ‘slow’ runs took a mean time of 124.2 seconds. Removing ‘zombie’ clusters saves computational time and memory usage associated with these parameters, and still gives exactly the same results.

Similar calculations show that setting  $r_{nk} = 0$  for removed clusters in MerDel with variable selection results in a similarly infinitesimally small approximation.

## H.3. ELBO calculation

We now look at each individual term in the ELBO. We set  $r_{nk} = 0$  for all  $n$  in removed clusters  $k$  and we show that are able to accurately calculate the ELBO after completely removing all values associated with cluster  $k$  from the model under this approximation.

### H.3.1. TERMS RULED BY $r_{nk}$

$$\mathbb{E}_{Z, \Phi}[\ln p(X|Z, \Phi)] = \sum_{n=1}^N \sum_{k=1}^K r_{nk} \left( \sum_{i=1}^D \mathbb{E}_{\Phi}[\ln \phi_{kix_{ni}}] \right) \quad (57)$$

$$\mathbb{E}_{Z, \pi}[\ln p(Z|\pi)] = \sum_{n=1}^N \sum_{k=1}^K r_{nk} \mathbb{E}_{\pi}[\ln \pi_k] \quad (58)$$

$$\mathbb{E}_Z[\ln q(Z)] = \sum_{n=1}^N \sum_{k=1}^K r_{nk} \ln r_{nk} \quad (59)$$

In all terms (57), (58), (59) all terms in the sums are multiplied by  $r_{nk}$ ; so all terms are equal to 0 for a removed cluster  $k$ . Removing terms associated with  $k$  has no effect.

H.3.2. TERMS RULED BY  $\Phi$ 

$$\mathbb{E}_{\Phi}[\ln p(\Phi)] = \sum_{k=1}^K \sum_{i=1}^D (-\ln B(\epsilon_{ki}) + \sum_{l=1}^{L_i} (\epsilon_{kil} - 1) \mathbb{E}_{\Phi}[\ln \phi_{kil}]) \quad (60)$$

$$= \sum_{k=1}^K \sum_{i=1}^D \mathbb{E}_{\Phi}[\ln p(\Phi_{kj})] \quad (61)$$

$$\mathbb{E}_{\Phi}[\ln q(\Phi)] = \sum_{k=1}^K \sum_{i=1}^D (-\ln B(\epsilon_{ki}^*) + \sum_{l=1}^{L_i} (\epsilon_{kil}^* - 1) \mathbb{E}_{\Phi}[\ln \phi_{kil}]) \quad (62)$$

$$= \sum_{k=1}^K \sum_{i=1}^D \mathbb{E}_{\Phi}[\ln q(\Phi_{kj})] \quad (63)$$

For the terms associated with  $\Phi$ , each cluster  $k$  is treated independently of one another. Each  $p(\Phi_{kj})$  prior and  $q(\Phi_{kj})$  variational posterior is a Dirichlet distribution of dimension  $L_j$ . We can therefore look at each  $(k, j)$  pair separately. For a removed cluster  $k$ , the  $\epsilon_{kj}^*$  values associated with that cluster are equal to the prior  $\epsilon_j$  values (Section H.1). Therefore we have, for a removed cluster  $k$ ,  $\mathbb{E}_{\Phi}[\ln p(\Phi_{kj})] - \mathbb{E}_{\Phi}[\ln q(\Phi_{kj})] = 0$ , as  $\epsilon_{kjl}^* = \epsilon_j$  for all  $k = 1, \dots, K, j = 1, \dots, P, l = 1, \dots, L_j$ . Ignoring cluster  $k$  in both the prior and variational posterior for  $\Phi$  therefore has no effect on the value of the ELBO.

 H.3.3. TERMS RULED BY  $\pi$ 

$$\mathbb{E}_{\pi}[\ln p(\pi)] = -\ln B(\alpha) + \sum_{k=1}^K (\alpha_k - 1) \mathbb{E}_{\pi}[\ln \pi_k] \quad (64)$$

$$\mathbb{E}_{\pi}[\ln q(\pi)] = -\ln B(\alpha^*) + \sum_{k=1}^K (\alpha_k^* - 1) \mathbb{E}_{\pi}[\ln \pi_k] \quad (65)$$

As in the previous section with  $\Phi$ , for a cluster  $k$ , we have that  $\alpha_k^* = \alpha_k = \alpha_0$ . Therefore, we have that the terms within the sums  $\sum_{k=1}^K (\alpha_k - 1) \mathbb{E}_{\pi}[\ln \pi_k]$  and  $\sum_{k=1}^K (\alpha_k^* - 1) \mathbb{E}_{\pi}[\ln \pi_k]$  associated with a removed cluster cancel each other out. This part of  $\mathbb{E}_{\pi}[\ln p(\pi)]$  and  $\mathbb{E}_{\pi}[\ln q(\pi)]$  can be considered safely dealt with.

However,  $\pi$  is a  $K$ -length vector modelled as a  $K$ -length Dirichlet distribution - both under the prior and in the variational posterior. When calculating  $\ln B(\alpha)$ ,  $\ln B(\alpha^*)$  and  $\mathbb{E}_{\pi}[\ln \pi_k]$ , we must take ‘zombie clusters’ into account.

$$-\ln B(\alpha) = \sum_{k=1}^K \ln \Gamma(\alpha_k) - \ln \Gamma\left(\sum_{k=1}^K \alpha_k\right) \quad (66)$$

$$\ln B(\alpha^*) = -\sum_{k=1}^K \ln \Gamma(\alpha_k^*) + \ln \Gamma\left(\sum_{k=1}^K \alpha_k^*\right) \quad (67)$$

We have that  $\ln \Gamma(\alpha_k)$  and  $\ln \Gamma(\alpha_k^*)$  inside the sums cancel each other out for a removed cluster  $k$ , as  $\alpha_k = \alpha_k^*$ . Therefore we need to take into account some  $\alpha, \alpha^*$  terms in  $\ln \Gamma(\sum \alpha_k)$ ,  $\ln \Gamma(\sum \alpha_k^*)$  which do not cancel out with each other. This is easily done by simply adding  $\alpha_0 \times K_{\text{rem}}$  into both sums over the  $\alpha, \alpha^*$  vectors, where  $\alpha_0$  is the parameter in the symmetric Dirichlet prior used for  $\pi$ , and  $K_{\text{rem}}$  is the number of clusters removed via merge/delete moves. This can be tracked trivially. A similar process must be used in calculating  $\mathbb{E}_{\pi}[\ln \pi_k]$ .

## H.4. Approximations and Priors in FedMerDel

There is no approximation when considering a ‘global merge’ in FedMerDel, as we never perform any variational E or M steps after performing merges. Our responsibilities  $r_{nk}$  remain exactly 0 for ‘zombie clusters’: given that we take the

zombie clusters into account when calculating the ‘global ELBO’ as above, we are okay to ‘remove’ empty clusters from the model parameters.

Note that as we enter the global setting, we define a new Dirichlet prior for  $\pi$  over our full dataset with the total number of local clusters initialised:  $B \times K_b$ , if  $K_b$  is the initialised number of clusters in Batch  $b$ . This is justified as each cluster has a prior where:

$$p(\pi) \propto \prod_{k=1}^K \pi_k^{\alpha_0 - 1} \tag{68}$$

with  $K$  representing the number of maximum clusters desired in the model. Therefore, when we enter the global setting with  $B$  batches, the maximum clusters in the model should be  $B \times K_b$ , the maximum total clusters when we consider all batches. A fractional prior for each batch would not be appropriate; this would be imposing a prior saying that there is a maximum number of  $K_b$  clusters across the full dataset, despite the fact we actually search for this number of clusters in each partition. We do not want to constrain the model to force all clusters to merge across batches; especially in the federated learning setting, there may be clusters appearing in certain batches of data but not other batches. This is consistent with similar literature; the same Dirichlet priors for mixing probabilities are used in ‘local clusters’ and ‘global clusters’ in (Zuanetti et al., 2018), a similar MCMC model to FedMerDel.

## I. Simulation Set-Up - Additional Information

### I.1. Data Generating Mechanism

We simulated synthetic binary data with  $N$  observations and  $P$  covariates by sampling the probability  $p$  of a ‘1’ in each cluster for each variable via a Beta(1, 5) distribution, encouraging sparse probabilities. For noisy variables, the probability of a ‘1’ was also generated by a Beta(1, 5) distribution but this probability was the same for every observation regardless of cluster membership. When simulating categorical data with  $L$  categories, we instead used a Dirichlet(1, ...,  $L$ ) distribution.

### I.2. Hyperparameter Choice

In all simulations (real-world and simulated data), we set  $\alpha_0 = 0.01$ ,  $\epsilon_j = 1/L_j$  and  $a = 2$  (as in Rao & Kirk (2024)) in the priors in Section 2 of the main paper. We did not tune these in this manuscript as all examples are purely illustrative. All algorithms were run with a maximum of 1000 iterations (an iteration being one variational EM step) - although this limit was not reached for any simulation.

Convergence tolerance was set between 0.000005 and 0.00000005 in all simulations. When comparing wall-clock time for convergence, all simulations in a given study had the exact same convergence tolerance.

In all simulations involving FedMerDel, we used the parameters ‘laps = 5’ for MerDel runs, except when explicitly specified.

### I.3. Frequency of Merge/Delete Moves

Details of the scenarios for this simulation study are given in Table 2 Simulations 1.1, 1.2, 1.3 were run without variable selection; Simulations 1.4, 1.5 were run with variable selection.  $K_{init}$  refers to the initialised value of  $K$  in the model. In each scenario, we generated 20 independent datasets and compared 10 different initialisations for each dataset.

Table 2. Table giving parameters for data generation for the first simulation study, ‘Frequency of Merge/Delete Moves’.

ID	RELEVANT VARIABLES	$N$	$P$	$K_{init}$	$K_{true}$	$N$ PER CLUSTER
1.1	100	1000	60	20	5	100-300
1.2	100	2000	100	20	8	50-800
1.3	100	4000	100	25	10	200-800
1.4	75	1000	100	20	10	50-200
1.5	60	1500	100	20	10	50-200

#### I.4. Global Merge Simulations

We aimed to evaluate the clustering performance of FedMerDel when splitting a simulated dataset into equally sized batches, and compared this to a parallelised version of MerDel (on the full dataset) as well as the usual MerDel algorithm on the full dataset (usual variational EM with merge and delete moves). We set ‘laps = 5’,  $P = 100$  covariates, 12 true clusters and 20 initialised clusters in all cases. Correlation was used for all merge criteria. These parameters were all kept the same to enable comparison of run-times between different values of  $N$ . Details of the values of  $N$  tested and number of batches/cores used are given in Table 3.

The full, unparallelised algorithm was only used for the first 4 simulations listed, as it became computationally infeasible for larger values of  $N$  with our hardware.

Table 3. Table giving parameters for data generation for the second simulation study, ‘Global Merge Simulations’, where other parameters are set as in Section I.4.

N	BATCHES/CORES
20000	5
50000	5
50000	10
100000	5
100000	10
200000	5
200000	10
500000	10

**K=6 simulations** We looked at some simulations with a lower number of ‘true clusters’ (6). All datasets had  $P = 100$  covariates, and we split these into 20 batches or parallelised over 20 cores. We initialised with 10 clusters in all MerDel cases. We compare FedMerDel to parallelised MerDel. We looked at  $N = 100,000$  and  $N = 500,000$ .

**Varying P** We additionally compared the ARI, number of clusters and the time taken for clustering models using parallelised MerDel and FedMerDel when we varied  $P$ . In this simulation, we simulated 5 synthetic datasets and ran MerDel and FedMerDel with 5 ‘shuffles’/initialisations each time. Datasets were all of size  $N = 100,000$  with 10 equally sized clusters, and we initialised with 20 clusters in all cases. We split into 5 equally sized batches for FedMerDel, and parallelised over 5 cores for parallelised MerDel. Results can be found in Appendix J.2.2.

**Global Merge with Variable Selection** For this simulation with variable selection (on binary data), we employed the ‘greedy search’ for the global merge, and used correlation to assess similarity between clusters. The two scenarios had simulated data split into 5 equally sized batches with  $N = 20,000, 50,000$ , with  $K = 15$  and 10 equally sized true clusters respectively. We set  $P = 100$  covariates in both cases, where 80% were relevant to the clustering structure in the first simulation and 75% were relevant in the second simulation. We generated 5 simulated datasets and had 5 different ‘shuffles’ of the data, as well as running MerDel on the full data 5 times (unparallelised and parallelised), as with other ‘global merge’ simulations in this manuscript.

As well as looking at ARI, number of resulting clusters and wall-clock time as with other simulations, we looked at the number of selected variables. As described in Section G, for FedMerDel, we consider a variable selected if it was selected in either all batches, or all but one batch (where a variable is selected if  $c_j > 0.5$ , the expectation of the variable selection latent variable (Appendix D)).

#### I.5. Number of Batches

With datasets of size  $N = 100,000$  and  $N = 200,000$ , we compared the clustering performance when considering  $B = 2, 4, 10$  and  $B = 4, 8, 20$  batches respectively. Batches were sized equally. We simulated 20 different synthetic datasets with  $P = 100$  for each scenario and took 5 different ‘shuffles’ of the data for every global merge model. Models had 10 unevenly sized ‘true’ clusters (cluster sizes ranging from 5% to 20% of the dataset) and were initialised with 20 clusters.

## J. Additional Simulation Results

### J.1. Frequency of Merge/Delete Moves

Tables comparing wall-clock time, final log-ELBO and ARI of the resulting clustering structures in Simulations 1.1, 1.2 and 1.3 are shown below (Tables 4, 5, 6).

Table 4. Table comparing the mean wall-clock time, mean final log-ELBO, mean ARI and mean number of clusters of the final labelling structure across all runs in Simulation 1.1 with confidence intervals for time and ARI (+- 1.96 x standard deviation).

LAPS	TIME (S)	LOG-ELBO	ARI	CLUSTERS
0	<b>3.46 [3.43, 3.49]</b>	-25357	0.856 [0.852, 0.860]	5.01
1	6.35 [6.16, 6.55]	<b>-25354</b>	<b>0.858 [0.854, 0.862]</b>	5.00
2	5.88 [5.75, 6.01]	<b>-25354</b>	<b>0.858 [0.854, 0.862]</b>	5.00
5	6.75 [6.65, 6.85]	<b>-25354</b>	<b>0.858 [0.854, 0.862]</b>	5.00
10	8.68 [8.57, 8.80]	<b>-25354</b>	<b>0.858 [0.854, 0.862]</b>	5.00
10000	14.0 [13.2, 14.7]	-25617	0.823 [0.818, 0.828]	15.3

Table 5. Table comparing the mean wall-clock time, mean final log-ELBO, mean ARI and mean number of clusters of the final labelling structure across all runs in Simulation 1.2 with confidence intervals for time and ARI (+- 1.96 x standard deviation).

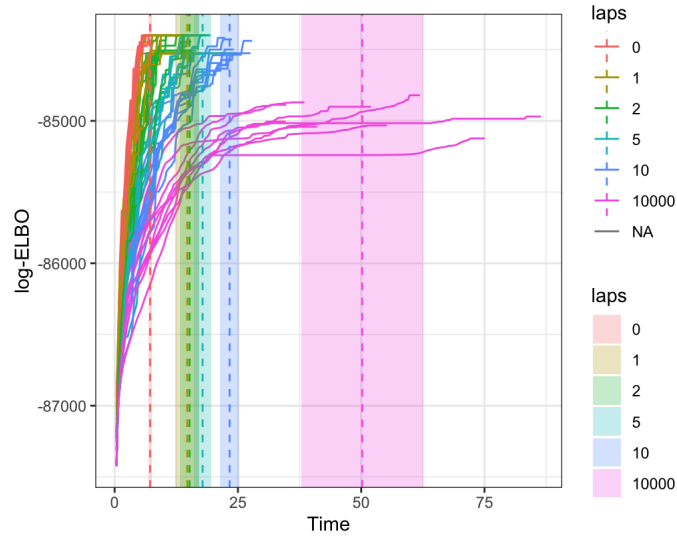
LAPS	TIME (S)	LOG-ELBO	ARI	CLUSTERS
0	<b>10.9 [10.8, 11.0]</b>	-81256	0.959 [0.957, 0.961]	7.65
1	29.1 [26.4, 31.8]	-81245	0.962 [0.960, 0.963]	7.63
2	23.4 [21.7, 25.1]	-81238	0.962 [0.961, 0.963]	7.70
5	25.4 [24.1, 26.7]	<b>-81236</b>	<b>0.963 [0.962, 0.964]</b>	7.84
10	31.0 [30.0, 32.0]	-81260	0.962 [0.961, 0.963]	8.54
10000	47.5 [45.0, 50.0]	-81721	0.940 [0.938, 0.942]	18.0

Table 6. Table comparing the mean wall-clock time, mean final log-ELBO, mean ARI and mean number of clusters of the final labelling structure across all runs in Simulation 1.3 with confidence intervals for time and ARI (+- 1.96 x standard deviation).

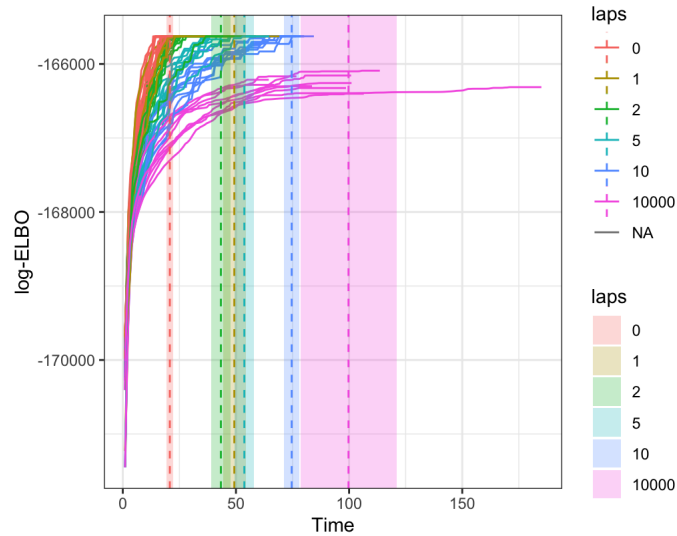
LAPS	TIME (S)	LOG-ELBO	ARI	CLUSTERS
0	<b>29.1 [28.8, 29.4]</b>	-164099	0.953 [0.952, 0.955]	10.0
1	57.1 [54.8, 59.5]	<b>-164090</b>	<b>0.954 [0.953, 0.955]</b>	10.0
2	52.1 [50.7, 53.5]	-164095	0.954 [0.952, 0.955]	10.0
5	61.8 [60.5, 63.1]	-164100	0.954 [0.952, 0.955]	10.2
10	76.5 [74.7, 78.3]	-164173	0.953 [0.951, 0.954]	12.0
10000	122 [112, 113]	-164675	0.943 [0.941, 0.944]	22.7

We can clearly see from Figure S1 that a) the original variational model clearly takes far longer than models with merge/delete b) there are steep improvements in ELBO near the start with more frequent merge/delete moves. However, for example, ‘laps = 1’ is near convergence very early on in both plots, but the algorithm takes longer to actually converge and stop.

Another observation we made, especially with Simulation 1.1, is that the variations of MerDel (laps between 1 to 10) frequently identified exactly the same model as one another and achieved higher ARIs than the variational models with no merge/delete moves. This could be indicative that the merge/delete moves are allowing the model to escape local optima and could be reaching a global optimum.



(a) Simulation 1.2



(b) Simulation 1.3

Figure S1. Graphs showing the ELBO vs wall-clock time for the algorithm for two simulated datasets across all 20 initialisations for each of the different "laps" in Simulations 1.2 and 1.3. The mean end time across all initialisations is shown as well as an approximate 95 confidence interval.

### J.1.1.1. VARIABLE SELECTION

Tables comparing wall-clock time, final log-ELBO, ARI and number of clusters of the resulting clustering structures in Simulations 1.4 and 1.5 are shown below (Tables 7, 8). We still see a speed up in terms of wall-clock time in these simulations, but see that there is more inconsistency with solutions with noisier data, especially as we increase the number of merge/delete moves, and the mean ARI for merge/delete models is generally lower when we incorporate more merge/delete moves. The number of clusters at convergence is also lower than the number we expect. We see from Figure S3 that it seems to be that merge/delete moves lead to less consistent results in the variable selection setting, but most of the best-performing models in terms of ARI are from MerDel models. As noted later (Section J.5.1), fewer clusters and lower ARIs in MerDel models could be an indication that some 'true' clusters could have been merged in the MerDel structures, if the 'true' clusters share similar characteristics.

However, the mean ELBO achieved by the resulting clustering models at convergence is still higher for all merge/delete



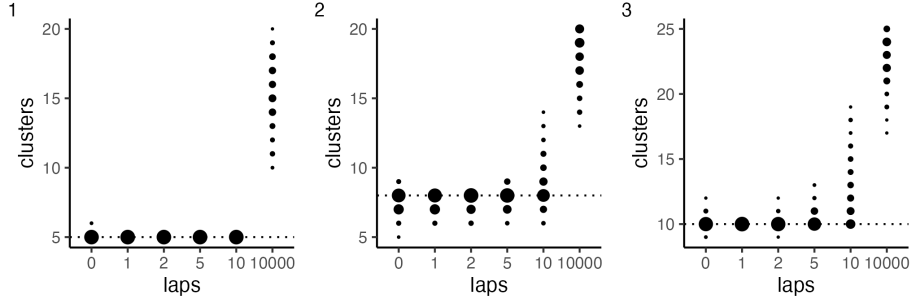


Figure S2. Plot comparing final number of clusters in clustering models in simulations 1.1-1.3.

models compared to the model with no merge/delete moves. This suggests that more care needs to be taken with the frequency of merge/delete moves used when including variable selection - it is likely that our merge/delete models are sometimes, for example, jumping too quickly to a model which has marked more variables as irrelevant and has fewer clusters, but does have a higher ELBO. MerDel models are still able to achieve some improved results, but these are more inconsistent.

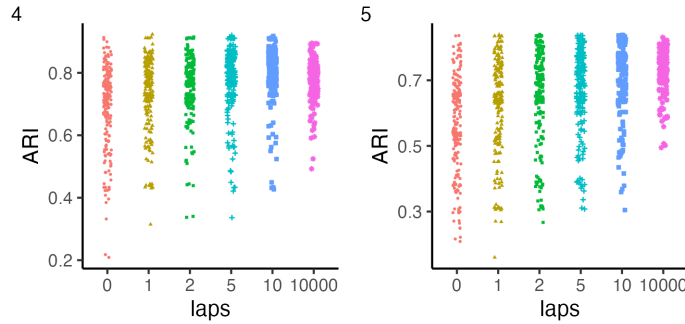


Figure S3. Scatter plot comparing ARIs achieved by each model across all datasets and initialisations in Simulations 1.4 and 1.5.

Table 7. Table comparing the mean wall-clock time, mean final log-ELBO, mean ARI and mean number of clusters of the final labelling structure across all runs in Simulation 1.4 with confidence intervals for time and ARI (+- 1.96 x standard deviation).

LAPS	TIME (S)	LOG-ELBO	ARI	CLUSTERS
0	<b>16.9</b> [16.6, 17.2]	-41913	0.692 [0.674, 0.710]	7.53
1	91.7 [84.0, 99.3]	-41848	0.731 [0.714, 0.747]	7.86
2	75.6 [69.8, 81.4]	-41838	0.753 [0.739, 0.767]	8.10
5	74.4 [70.0, 78.7]	<b>-41823</b>	0.773 [0.759, 0.787]	8.48
10	92.7 [88.4, 96.9]	-41831	<b>0.792</b> [0.780, 0.804]	9.16
10000	128 [118, 138]	-42372	0.782 [0.774, 0.791]	19.3

We additionally used  $F_1$  scores to compare the quality of variable selection. Having merge/delete moves tends to improve the quality of the variable selection as quantified by  $F_1$  scores compared to the model with no merge/delete moves. This is illustrated in Table 9 with results from Simulation 1.4 shown. The gains are made especially in terms of identifying irrelevant, noisy variables, and laps 2 and 5 get the top  $F_1$  scores of 0.977, indicating extremely good feature selection performance. Overall, although there is some desire for improvement in accuracy for the clustering structure when implementing variable selection, we see that merge and delete moves make improvements in identifying relevant clustering variables.

Table 8. Table comparing the mean wall-clock time, mean final log-ELBO, mean ARI and mean number of clusters of the final labelling structure across all runs in Simulation 1.5 with confidence intervals for time and ARI (+- 1.96 x standard deviation).

LAPS	TIME (S)	LOG-ELBO	ARI	CLUSTERS
0	<b>24.0 [23.7, 24.4]</b>	-61781	0.561 [0.540, 0.581]	6.60
1	137 [125, 149]	-61664	0.625 [0.605, 0.645]	7.29
2	110 [101, 118]	-61640	0.651 [0.631, 0.670]	7.67
5	112 [107, 118]	-61622	0.679 [0.661, 0.696]	8.12
10	149 [143, 156]	<b>-61612</b>	0.710 [0.695, 0.725]	8.90
10000	213 [199, 227]	-62204	<b>0.730 [0.721, 0.739]</b>	19.3

Table 9. Table comparing the mean  $F_1$  scores, and number of relevant and irrelevant variables successfully found across all simulated datasets and all initialisations in Simulation 1.4 and Simulation 1.5.

LAPS	SIMULATION 1.4			SIMULATION 1.5		
	REL	IRREL	$F_1$ SCORE	REL	IRREL	$F_1$ SCORE
0	73.4	21.7	0.968	58.8	34.6	0.947
1	73.5	<b>22.7</b>	0.975	58.7	<b>36.0</b>	0.957
2	73.9	<b>22.7</b>	<b>0.977</b>	59.2	35.8	<b>0.959</b>
5	74.0	22.4	<b>0.977</b>	<b>59.3</b>	35.5	0.958
10	74.0	22.2	0.975	<b>59.3</b>	34.9	0.954
10000	<b>74.1</b>	15.5	0.935	<b>59.3</b>	23.1	0.872

**J.2. Global Merge Simulations - Additional Results**

Table 10. ‘Global Merge Simulations’ results. We report the median and lower/upper quantiles across all 10 ‘shuffles’/initialisations and all 10 synthetic datasets. FedMerDel/G is the greedy search, FedMerDel/R is the random search for FedMerDel. Note separate independent datasets were generated for  $N$  equal but different numbers of batches/cores, accounting for slight differences in ARI.

N	MODEL	BATCHES/CORES	ARI	CLUSTERS	TIME (S)
20000	FULL	5	0.943 [0.933, 0.950]	12 [11.8, 12]	106 [92.8, 130]
	PAR	5	0.943 [0.930, 0.950]	12 [11, 12]	37.0 [33.4, 40.6]
	FEDMERDEL/G	5	0.920 [0.912, 0.933]	12 [12, 12]	33.1 [28.9, 37.2]
	FEDMERDEL/R	5	0.920 [0.912, 0.932]	12 [12, 12]	33.2 [29.1, 37.4]
50000	FULL	5	0.947 [0.941, 0.954]	12 [12, 12]	467 [414, 554]
	PAR	5	0.948 [0.942, 0.954]	12 [12, 12]	176 [163, 196]
	FEDMERDEL/G	5	0.945 [0.939, 0.949]	13 [13, 14]	114 [106, 123]
	FEDMERDEL/R	5	0.945 [0.939, 0.948]	12 [12, 12]	114 [106, 123]
50000	FULL	10	0.957 [0.955, 0.958]	12 [12, 12]	465 [432, 512]
	PAR	10	0.956 [0.955, 0.958]	12 [12, 12]	126 [121, 142]
	FEDMERDEL/G	10	0.951 [0.946, 0.954]	13 [13, 14]	70.6 [66.2, 75.8]
	FEDMERDEL/R	10	0.951 [0.946, 0.954]	12 [12, 13]	71.3 [66.8, 76.6]
100000	FULL	5	0.955 [0.944, 0.961]	12 [12, 12]	956 [861, 1116]
	PAR	5	0.954 [0.944, 0.961]	12 [12, 12]	338 [310, 380]
	FEDMERDEL/G	5	0.954 [0.943, 0.960]	13 [12, 13]	260 [231, 287]
	FEDMERDEL/R	5	0.954 [0.943, 0.960]	12 [12, 12]	260 [232, 287]
100000	PAR	10	0.949 [0.941, 0.959]	12 [12, 12]	249 [231, 284]
	FEDMERDEL/G	10	0.948 [0.938, 0.952]	13 [13, 14]	131 [123, 143]
	FEDMERDEL/R	10	0.948 [0.938, 0.952]	12 [12, 13]	132 [124, 144]
200000	PAR	10	0.952 [0.947, 0.958]	12 [12, 12]	482 [446, 536]
	FEDMERDEL/G	10	0.951 [0.946, 0.957]	13 [13, 14]	269 [242, 303]
	FEDMERDEL/R	10	0.951 [0.946, 0.957]	12.5 [12, 13]	270 [243, 305]
500000	PAR	10	0.950 [0.943, 0.951]	12 [12, 12]	1121 [1056, 1303]
	FEDMERDEL/G	10	0.949 [0.942, 0.951]	13 [13, 14]	685 [642, 793]
	FEDMERDEL/R	10	0.949 [0.942, 0.951]	12.5 [12, 13]	688 [646, 797]
1000000	PAR	20	0.948 [0.943, 0.953]	12 [12, 12]	2119 [2031, 2204]
	FEDMERDEL/G	20	0.948 [0.943, 0.953]	13.5 [13, 14]	899 [825, 984]
	FEDMERDEL/R	20	0.948 [0.943, 0.953]	14 [13, 14]	912 [840, 1007]

**J.2.1. K=6 SIMULATIONS**

Similar results were seen as with the simulation scenarios with  $K = 12$ , where the gains in time efficiency from using FedMerDel instead of parallelised MerDel increased as  $N$  increased.

Table 11. Results from ‘Global Merge Simulations’ with  $K = 6$  clusters, where all datasets have  $P = 100$  covariates, and are split into 20 batches or parallelised over 20 cores. We initialised with 10 clusters in all MerDel cases. We compare FedMerDel to parallelised MerDel. We report the median and lower/upper quantiles across 5 ‘shuffles’/initialisations for 5 synthetic datasets. Results are for the random search; greedy searches differed insignificantly.

N	MODEL	ARI	CLUSTERS	TIME (S)
100000	PAR	0.974 [0.967, 0.978]	6 [6, 6]	111 [103, 121]
	FEDMERDEL	0.965 [0.972, 0.977]	6 [6, 6]	70.5 [66.2, 77.6]
500000	PAR	0.970 [0.969, 0.975]	6 [6, 6]	645 [619, 734]
	FEDMERDEL	0.970 [0.969, 0.975]	6 [6, 6]	455 [404, 516]

J.2.2. VARYING P

We saw a similar pattern to  $N$  where as  $P$  increases, the gains made from FedMerDel are increased compared to parallelised MerDel.

Table 12. ‘Global Merge Simulations’ results, where all datasets are of size  $N = 100,000$  (split into 5 batches/parallelised over 5 cores) and have 10 equally sized clusters, but  $P$  (number of covariates) is varied. We compare FedMerDel to parallelised MerDel. We report the median and lower/upper quantiles across 5 ‘shuffles’/initialisations for 5 synthetic datasets. Results are for the random search; greedy searches differed insignificantly.

P	MODEL	ARI	CLUSTERS	TIME (S)
60	PAR	0.782 [0.753, 0.796]	10 [10, 10]	206 [194, 231]
	FEDMERDEL	0.780 [0.751, 0.794]	10 [10, 10]	153 [130, 169]
80	PAR	0.874 [0.872, 0.880]	10 [10, 10]	285 [256, 333]
	FEDMERDEL	0.872 [0.870, 0.879]	10 [10, 10]	190 [182, 231]
120	PAR	0.972 [0.972, 0.973]	10 [10, 10]	316 [292, 345]
	FEDMERDEL	0.972 [0.971, 0.972]	10 [10, 10]	208 [203, 229]
200	PAR	0.999 [0.999, 0.999]	10 [10, 10]	465 [453, 469]
	FEDMERDEL	0.999 [0.999, 0.999]	10 [10, 10]	295 [291, 302]

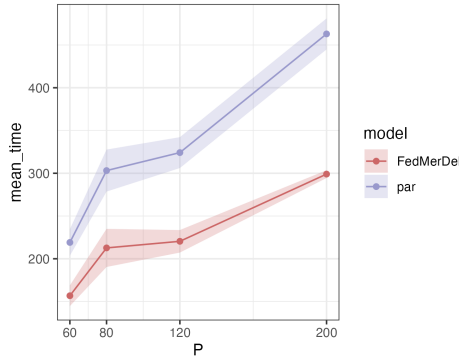


Figure S4. Plot comparing the mean time taken by parallelised MerDel (‘par’) and FedMerDel (‘shard’) as we vary  $P$ , with a 95% confidence interval ( $\text{mean} \pm 1.96 \times \frac{s.d.}{\sqrt{n}}$ ). Results for FedMerDel are with the greedy search, although there is no visible difference for the random search.

J.2.3. GLOBAL MERGE WITH VARIABLE SELECTION

Results showed similar performance in terms of ARI between FedMerDel and MerDel on the full dataset (Table 13). In these scenarios (with relatively low  $N$ ) FedMerDel did not outperform parallelised MerDel in terms of wall-clock time, but notably was almost always able to correctly identify relevant and irrelevant variables, outperforming both other methods, which usually wrongly identified some irrelevant variables as relevant. Global merge times were less than one second in all cases.

J.3. Number of Batches

Detailed results from this simulation study can be found in Table 14 and Figure S5. A Kruskal-Wallis test testing for any significant difference between the ARI for different numbers of batches for  $N = 100,000$  gives a p-value of 0.125. For  $N = 200,000$ , the p-value is 0.0938. One way to potentially improve inference for the number of clusters for higher values of  $K_{\text{init}}$  would be to look at higher frequencies of merge/delete moves within each MerDel run.

Table 13. ‘Global Merge with Variable Selection’ simulation results. We report the median and lower/upper quantiles across all 5 ‘shuffles’/initialisations and all 5 synthetic datasets. Global merge uses the ‘greedy search’. ‘Rel’ and ‘Irrel’ refer to the number of correctly identified relevant and irrelevant covariates respectively.

$N$	MODEL	ARI	CLUSTERS	TIME (S)	REL	IRREL
20000	FULL	0.865 [0.862, 0.868]	15 [15, 15]	782 [687, 835]	80 [80, 80]	18 [17, 18]
	PAR	0.865 [0.862, 0.868]	15 [15, 15]	207 [187, 228]	80 [80, 80]	17 [16, 17]
	FEDMERDEL	0.850 [0.844, 0.857]	15 [15, 15]	223 [212, 242]	80 [80, 80]	20 [20, 20]
50000	FULL	0.885 [0.876, 0.885]	10 [10, 10]	1607 [1493, 1767]	75 [75, 75]	23 [22, 24]
	PAR	0.885 [0.876, 0.886]	10 [10, 10]	462 [440, 527]	75 [75, 75]	23 [22, 24]
	FEDMERDEL	0.881 [0.873, 0.883]	10 [10, 10]	630 [563, 672]	75 [75, 75]	25 [25, 25]

Table 14. ‘Number of Batches’ simulation results. We report the median and lower/upper quantiles across all 5 ‘shuffles’ for each of the 20 synthetic datasets. Results use the random search for the global merge; there were only marginal differences for the greedy search.

$N$	BATCHES	ARI	CLUSTERS
100000	2	0.956 [0.950, 0.960]	10 [10, 10]
100000	4	0.955 [0.951, 0.960]	10 [10, 10]
100000	10	0.955 [0.951, 0.959]	10 [10, 11]
200000	4	0.954 [0.946, 0.959]	10 [10, 10]
200000	8	0.954 [0.946, 0.959]	10 [10, 10]
200000	20	0.953 [0.944, 0.958]	10 [10, 11]

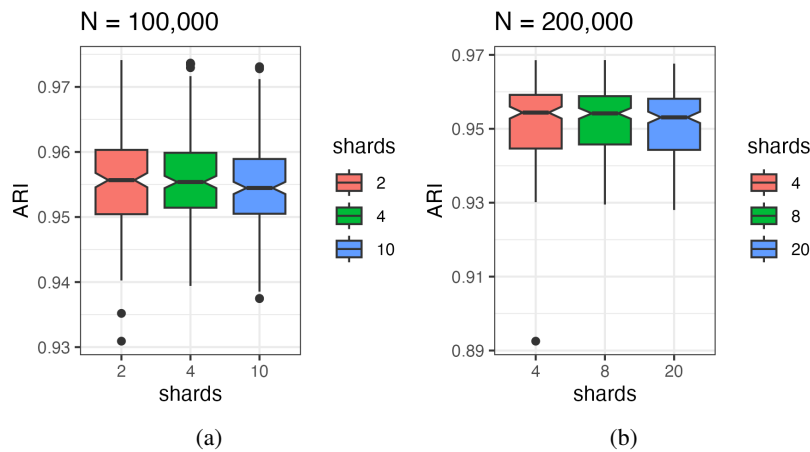


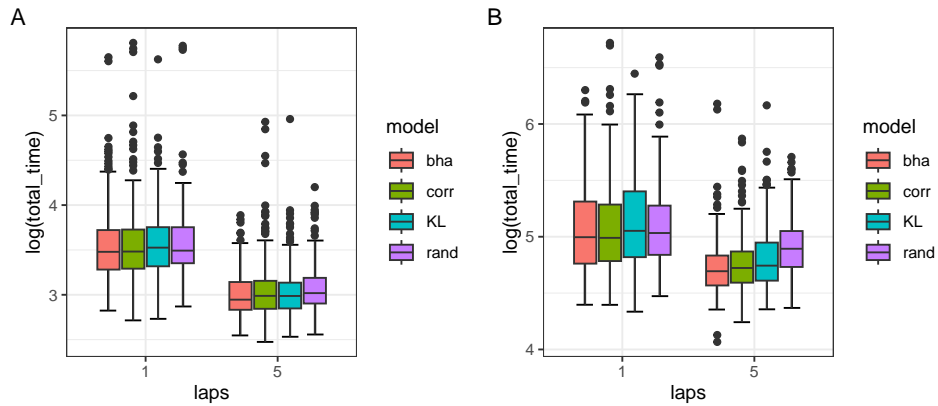
Figure S5. Boxplot showing the distribution of ARI scores across different numbers of batches in the ‘Number of Batches’ simulation.

#### J.4. Comparing Merge Criteria

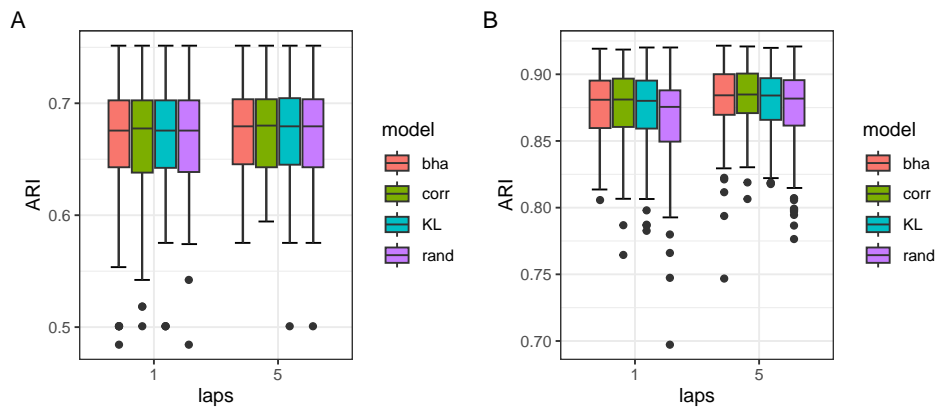
In this simulation, we compared methods of selecting candidate clusters for merging as described in Section E.1.1. We compared a correlation measure (‘corr’) and two divergence-based measures (Kullback-Leibler divergence, ‘KL’, and the Bhattacharyya distance, ‘bha’) to completely random selection of candidate clusters (‘rand’).

We ran two simulation studies: one with  $N = 2000$ ,  $K_{\text{true}} = 10$ ,  $K_{\text{init}} = 20$  and  $P = 50$  (A in Figure S6), and one with  $N = 2000$ ,  $K_{\text{true}} = 20$ ,  $K_{\text{init}} = 40$  and  $P = 100$  (B in Figure S6). In both cases, we simulated 30 independently generated binary datasets. For each dataset and each model, we ran the model 10 times with a different initialisation each time (giving 40 initialisations per dataset, and 10 per model). For each initialisation, we tested  $\text{laps} = \{1, 5\}$ .

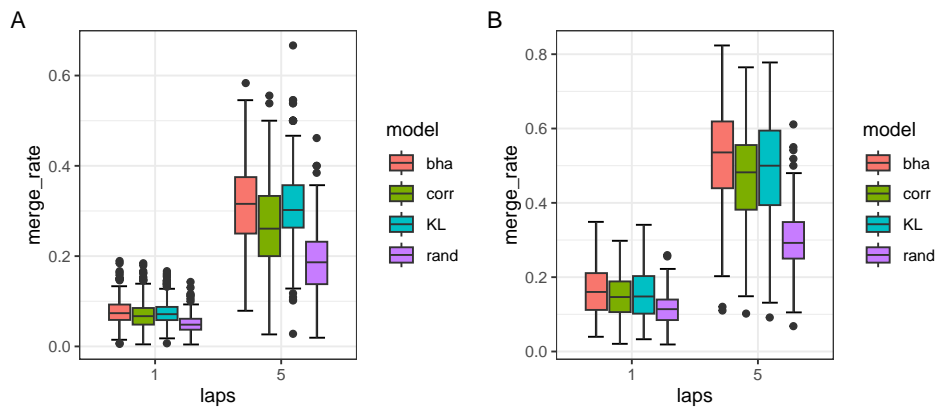
Figure S6 illustrates that generally, there was not a significant difference between the choice of methods to select candidate clusters for merging in terms of time and accuracy, although as expected, random choice did tend to take slightly longer - especially for  $\text{laps} = 5$  and in the dataset with more clusters. In plot B in Figure S6(b), the median of the ARIs achieved by ‘rand’ is slightly lower than other methods with both  $\text{laps} = 1$  and 5. We saw that the proportion of accepted merges was significantly lower than all other methods with random choice in most cases, and that ‘corr’ saw slightly lower merge rates than divergence-based measures. However, the computational complexity of calculating divergences is higher, leading to similar total times for the overall algorithm in Figure S6(a).



(a) Comparing log(total time (s))



(b) Comparing ARI



(c) Comparing 'merge rate', defined as proportions of merges accepted.

Figure S6. Boxplots comparing the distributions of ARI scores, (the logarithm of) total wall-clock time until convergence, and 'merge rates'. All initialisations for each model, simulated dataset and 'laps' value are included, where the boxplots illustrate the median, quantiles and range across all clustering solutions.

### J.5. Categorical Data Simulations

#### J.5.1. FREQUENCY OF MERGE/DELETE MOVES

Details of the scenarios for this simulation study with categorical data (analogous to Section I.3) are given in a table below. Both simulations were run without variable selection.  $K_{init}$  refers to the initialised value of  $K$  in the model. In both scenarios, we generated 20 independent datasets and compared 10 different initialisations for each dataset.

Table 15. Table giving parameters for data generation for the frequency of merge/delete moves with categorical data.

ID	$N$	$P$	$K_{init}$	$K_{true}$	$N$ PER CLUSTER	CATEGORIES
CAT.1	2000	100	20	8	50-800	4
CAT.2	4000	100	25	10	200-800	3

Tables comparing wall-clock time, final log-ELBO and ARI of the resulting clustering structures in Simulations cat.1, and cat.2 are shown below (Tables 16, 17).

It is notable that the model with no merge/delete moves (laps = 10000) performed significantly worse in terms of ARI in these simulations, especially when we increased the number of categories in each covariate (ie. in Simulation cat.1 with 4 categories). We also saw in both simulations that the fully variational model never ended with fewer clusters than the initialisation, which could suggest that the lower ARI could be associated with observations remaining in smaller clusters which are subsets of the original clusters. ARI scores only take into account pairwise clustering similarity; one cluster being split into multiple subclusters in another clustering result will result in the two clustering structures sharing a relatively low ARI, due to observations being in different clusters, even though it is a subcluster of the original cluster.

A brief inspection of the resulting clustering structures in Simulation cat.1 (for example) provided further evidence to this effect, where many of the 20 clusters contained more than just a few ‘left-out’ observations. In Simulation cat.1, the very uneven true cluster sizes could have also contributed to this effect. This further supports the usefulness of merge/delete moves in MerDel when applied to categorical data; these moves clearly help to mitigate poor optima and find a number of clusters closer to the truth.

Figure S9 illustrates the change in ELBO versus time for one simulated dataset for both categorical simulations. It is clear in these graphs that MerDel is able to converge at a ‘better’ local optima of the optimisation surface (ie. one with a higher ELBO) compared to the usual variational algorithm.

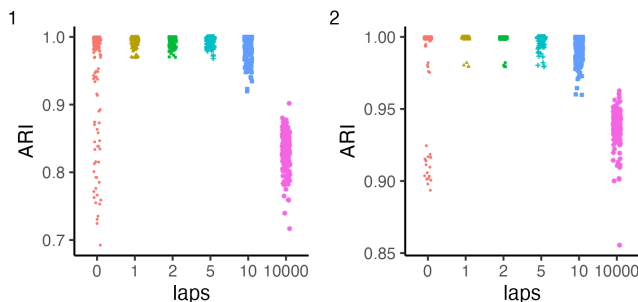


Figure S7. Scatter plot comparing ARIs achieved by each model across all datasets and initialisations in Simulations cat.1 and cat.2 (labelled 1, 2 respectively). Each point represents one ARI from one MerDel run.

#### J.5.2. GLOBAL MERGE SIMULATIONS

For this simulation with categorical data, we employed the ‘random search’ for the global merge and used the KL divergence to assess similarities between clusters in both the local merge move and the global merge (recall in the binary simulation, we used correlation). The three scenarios had simulated data with  $N = 20,000, 50,000, 100,000$ , with  $K = 20, 10$  and  $12$  true clusters split into 4, 5 and 5 equally sized batches respectively. We set  $P = 100$  covariates and 3 categories in each



covariate in all cases. We generated 5 simulated datasets and had 10 different ‘shuffles’ of the data in each scenario, as well as running MerDel and parallelised MerDel on the full data 10 times, as with the binary simulations.

Results showed extremely good performance with almost perfect clustering structures whether or not we employed a global merge or not in all cases. There was a clear speed up for the global merge model and for parallelised MerDel, and as we saw with binary data, as the data size increased, we saw increased gains from using FedMerDel as opposed to parallelising MerDel stepwise. Note the higher merge times and total times with  $N = 20,000$  were likely a result of the increased number of true clusters and initialised clusters in each MerDel run (30). In the later two simulations, we initialised with 20 clusters.

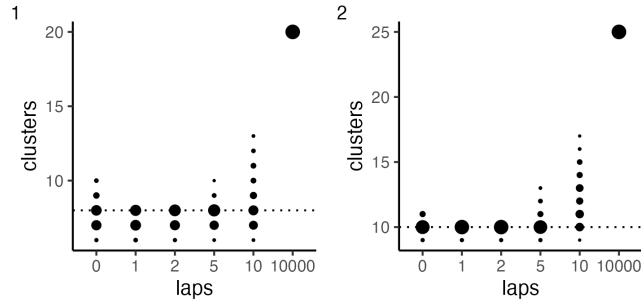


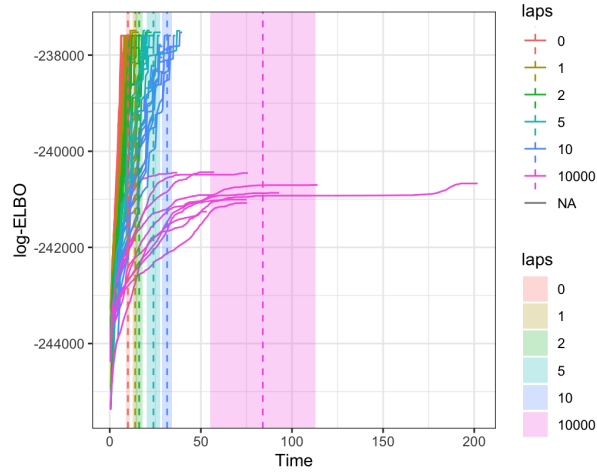
Figure S8. Plot comparing final number of clusters in clustering models in simulations cat.1 and cat.2.

Table 16. Table comparing the mean wall-clock time, mean final log-ELBO, mean ARI and mean number of clusters of the final labelling structure across all runs in Simulation cat.1 with confidence intervals for time and ARI (+- 1.96 x standard deviation).

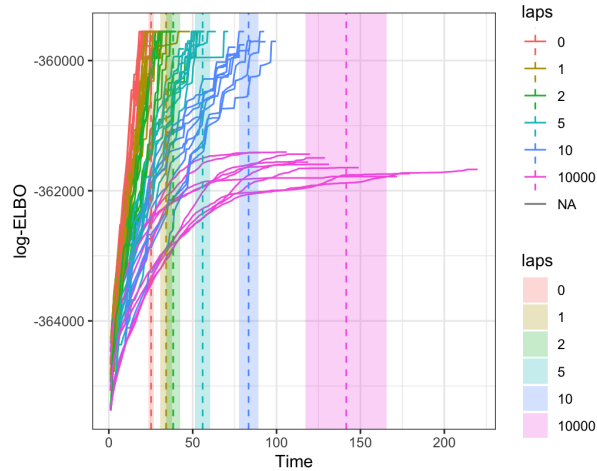
LAPS	TIME (S)	LOG-ELBO	ARI	CLUSTERS
0	<b>14.4</b> [14.2, 14.5]	-238524	0.961 [0.951, 0.971]	7.72
1	27.6 [25.6, 29.5]	-238378	0.994 [0.993, 0.995]	7.48
2	24.5 [23.1, 25.8]	-238356	<b>0.995</b> [0.994, 0.996]	7.56
5	29.2 [28.5, 29.8]	<b>-238352</b>	<b>0.995</b> [0.994, 0.996]	7.71
10	38.7 [37.8, 39.5]	-238513	0.986 [0.984, 0.988]	8.37
10000	79.2 [74.6, 83.8]	-241501	0.831 [0.827, 0.835]	20

Table 17. Table comparing the mean wall-clock time, mean final log-ELBO, mean ARI and mean number of clusters of the final labelling structure across all runs in Simulation cat.2 with confidence intervals for time and ARI (+- 1.96 x standard deviation).

LAPS	TIME (S)	LOG-ELBO	ARI	CLUSTERS
0	<b>34.8</b> [34.1, 35.4]	-360586	0.991 [0.988, 0.995]	10.1
1	47.0 [46.0, 48.1]	<b>-360544</b>	<b>0.999</b> [0.999, 1.00]	10.0
2	49.8 [48.8, 50.7]	<b>-360544</b>	<b>0.999</b> [0.999, 1.00]	10.0
5	66.1 [65.1, 67.0]	-360568	0.998 [0.998, 0.999]	10.2
10	91.1 [89.5, 92.8]	-360795	0.991 [0.990, 0.992]	12.1
10000	172 [162, 181]	-312628	0.939 [0.937, 0.941]	25



(a) Simulation cat.1



(b) Simulation cat.2

Figure S9. Graphs showing the ELBO vs wall-clock time for the algorithm for two simulated datasets across all 20 initialisations for each of the different "laps" in Simulations cat.1 and cat.2. The mean end time across all initialisations is shown as well as an approximate 95 confidence interval.

Table 18. 'Global Merge Simulations' with categorical data results. We report the median and lower/upper quantiles across all 10 'shuffles'/initialisations and all 5 synthetic datasets.

$N$	MODEL	ARI	CLUSTERS	TIME (s)	GLOBAL MERGE TIME (s)
20000	FULL	0.999 [0.999, 0.999]	20 [20, 20]	387 [373, 418]	
	PAR	0.999 [0.999, 0.999]	20 [20, 21]	146 [128, 157]	
	FEDMERDEL	0.998 [0.99, 0.998]	20 [20, 20]	124 [118, 131]	3.91 [3.82, 4.14]
50000	FULL	0.999 [0.999, 1.00]	10 [10, 10]	374 [373, 375]	
	PAR	0.999 [0.999, 1.00]	10 [10, 10]	127 [125, 128]	
	FEDMERDEL	0.999 [0.999, 1.00]	10 [10, 10]	83.5 [80.7, 84.1]	1.29 [1.28, 1.34]
100000	FULL	1.00 [0.999, 1.00]	12 [12, 12]	946 [857, 1050]	
	PAR	1.00 [0.999, 1.00]	12 [12, 12]	293 [276, 339]	
	FEDMERDEL	0.999 [0.990, 1.00]	12 [12, 13]	243 [219, 280]	2.57 [2.49, 2.64]

## K. MNIST - Additional Results

### K.1. Supplementary Figures

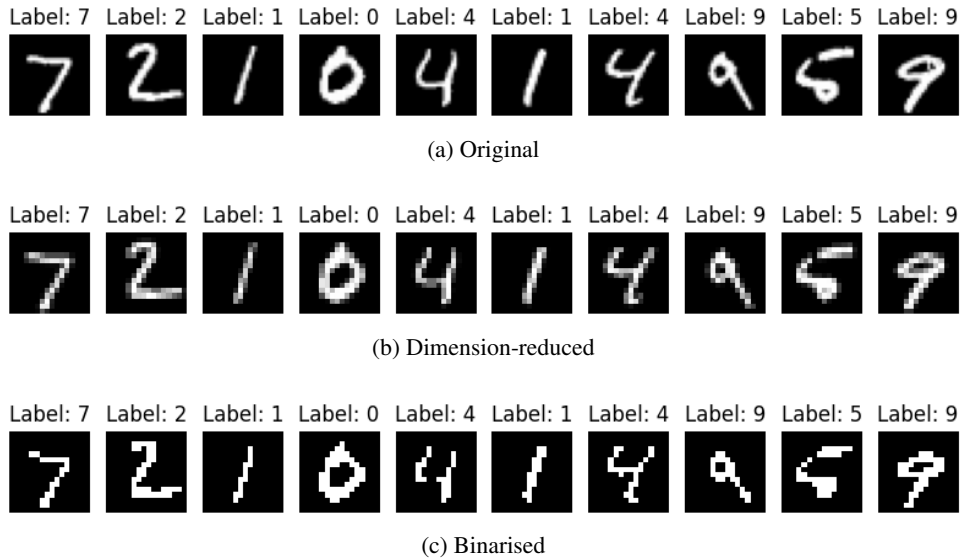


Figure S10. Example of the first 10 MNIST test-set digits visualised in their original image format (28x28), the same digits with the dimensionality reduction applied (16x16), and the same dimension reduced digits converted to a binary format.

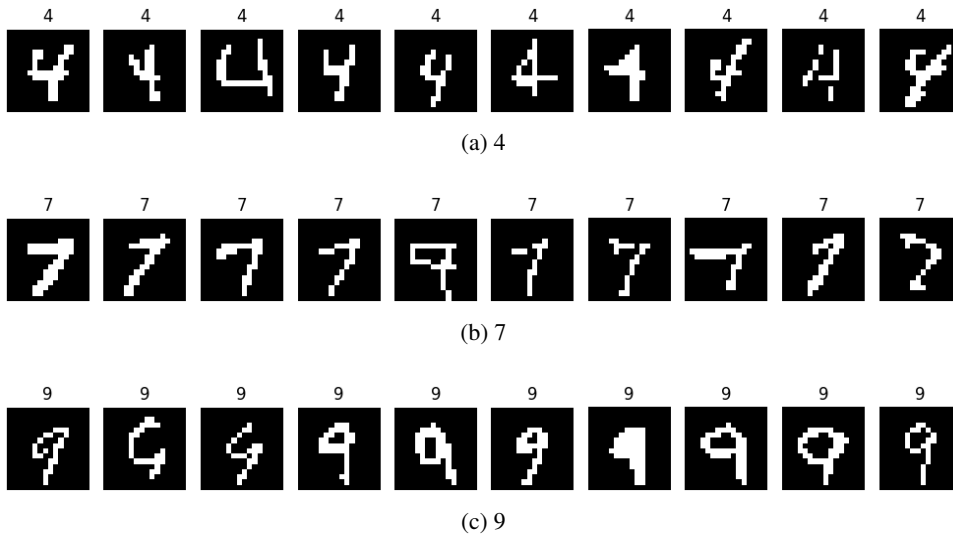


Figure S11. 10 randomly selected digits of 4, 7 and 9 from the MNIST dataset, showing similarities in their shapes.

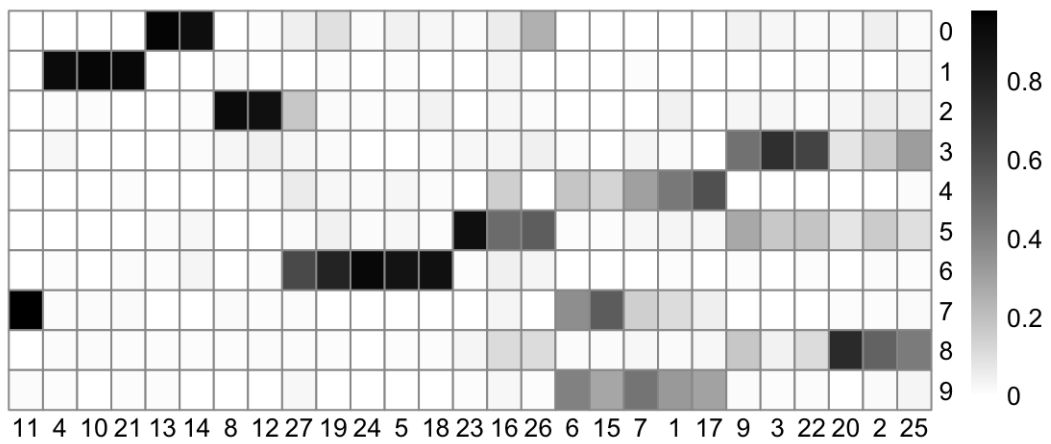
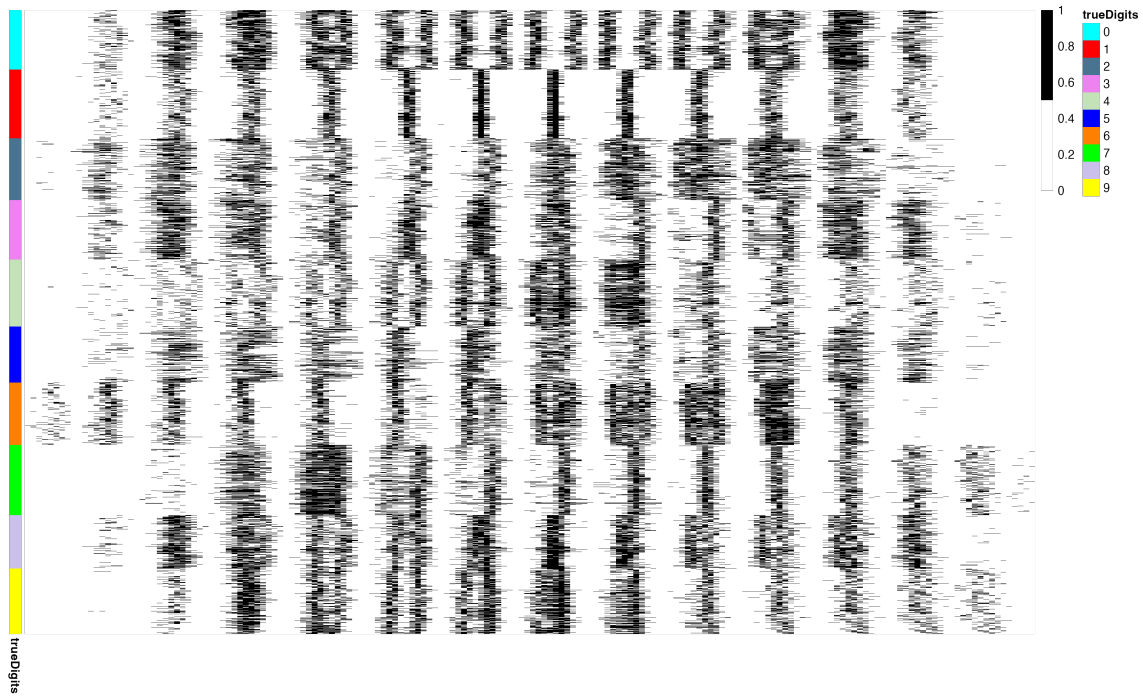
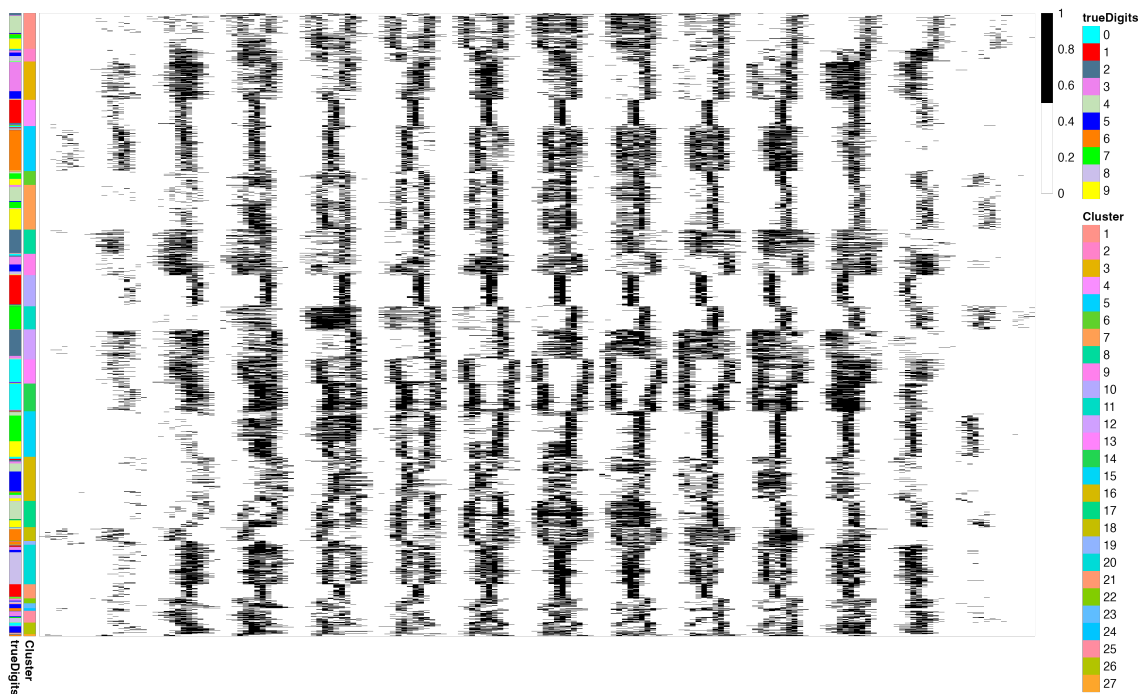


Figure S12. A heatmap showing the correspondence between clusters and true numbers in the clustering model with the best ELBO for the MNIST data. A darker cell colour in entry  $(i, j)$  indicates a higher percentage of samples from number  $i$  are in the given cluster  $j$ . The exact number corresponds to the percentage of cluster  $j$  made up of the given number.

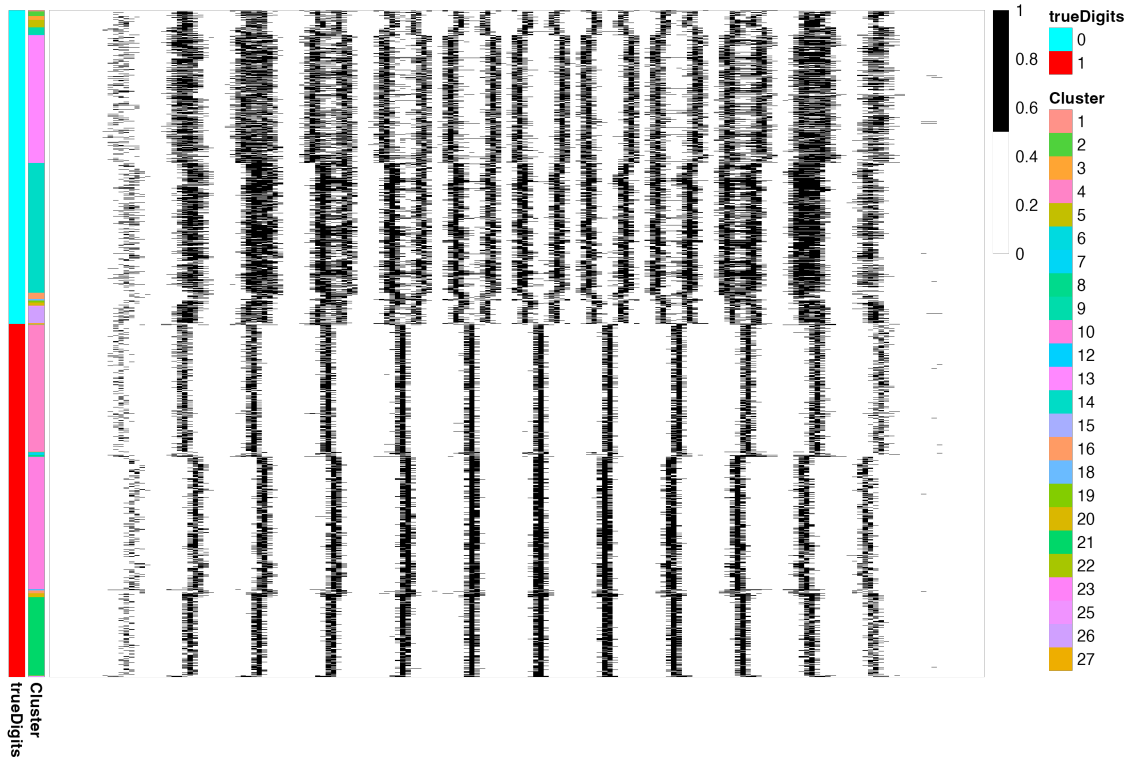


(a) Sorted by true digits

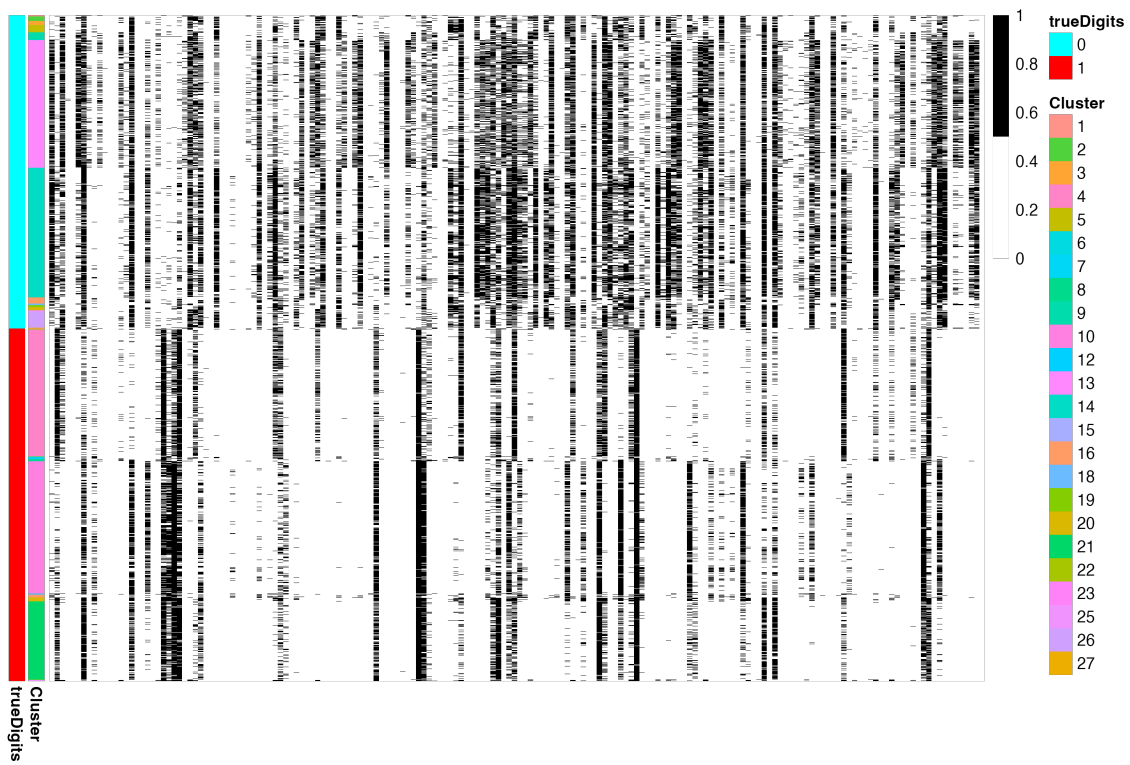


(b) Sorted by cluster

Figure S13. Heatmaps showing the first 2000 digits in our pre-processed MNIST dataset, first sorted by true digit and then sorted by cluster for the clustering model with the best ELBO. Differences between and within digits can be seen.



(a) Columns in default order



(b) Columns shuffled

Figure S14. Heatmaps showing only 0's and 1's in the first 10000 digits in our pre-processed MNIST dataset, sorted by cluster within both digits. Shuffling the columns allows the differences between separate clusters to be clearer.

## K.2. Supplementary Results - Classification Rates

In Table 19, the models included are:

- **FedMerDel\_rand**: Our novel federated learning model, FedMerDel, analysed in the main paper. This included 6 equally sized batches of data with 20 maximum clusters in each batch. A random search was used for the global merge. All models took between 77-126 mins.
- **FedMerDel\_greedy**: FedMerDel, but with a greedy search used for the global merge. The same batches were used as with FedMerDel\_random above. All models took between 77-127 minutes.
- **FedMerDel\_30r**: FedMerDel with 6 equally sized batches of data, but now with 30 maximum clusters in each batch. These models had slightly better classification rates, but came at a high cost of computational time with 60 extra clusters being processed, and reduced scope for interpretation of clusters. Resulting models had between 52-70 clusters. More clusters than 30 per batch could be used if an even finer and robust clustering structure is desired, but this was not the aim of our analysis, where we focused on finding a broad clustering structure with a large dataset to validate the scalability of our method. This model used a random search.
- **FedMerDel\_30g**: Same model and batches as above, but with a greedy search. These models had between 52-61 clusters.
- **kmeans\_xx\_yy**: In this model, in order to implement scalable clustering methods for continuous data to compare to, we projected the data to a lower dimension with Multiple Correspondence Analysis (MCA), a counterpart to principal component analysis for categorical data. We then implement the k-means algorithm on this lower-dimensional data. xx represents the number of MCA dimensions kept in the model, which is 5 (explaining 20% of variance), 10 (explaining 30% of variance) or 17 (explaining 40% of variance). yy represents the number for  $k$ , the number of clusters, where we test 20 and 35. In all cases, we use 20 maximum iterations for k-means, and 20 different initialisations, and use the clustering with the best total within-cluster sum of squares. We saw that this method is quick (taking no longer than a minute) and generally performs well especially as we increase the number of dimensions and clusters, although does not separate numbers such as 2, 3 and 6 as well as our models.
- **EM\_yy**: We applied an EM algorithm for frequentist model estimation to fit a finite mixture model to the MNIST binary data via the R package *flexmix* (Leisch, 2004) and used the BIC (Bayesian Information Criterion) for model selection across a given number of initialisations. yy represents the number of clusters in the finite mixture model, and we test 20 (10.2 mins) and 35 (55.4 mins). We use 10 different initialisations, and the model returned is the maximum likelihood solution.
- **MCA\_EM\_yy**: We also applied an EM algorithm to fit a Gaussian mixture model to MCA-transformed MNIST data. For this, we used the R package *mclust* which also uses the BIC to select the optimal model between 14 models with different shapes, volumes, and orientations of covariances. yy represents the number of clusters in the finite mixture model, and we test 20 (4.45 mins) and 35 (9.77 mins).

Generally, FedMerDel performed similarly well to comparator methods, where 0's, 1's, 2's and 6's saw higher classification rates with methods such as EM.

Table 19. Table comparing classification rates (%) for each digit across different clustering models. The model analysed further in the paper and supplement was the 4th FedMerDel\_rand run as the model with the highest ELBO of all the FedMerDel\_rand and FedMerDel\_greedy runs. Classification rate is defined as the percentage of digits classified into a cluster primarily consisting of that digit.

MODEL	RUN	0	1	2	3	4	5	6	7	8	9
FedMerDel_rand	1	83.4	95.5	83.7	75.5	49.6	37.8	90.4	62.2	65.6	<b>55.3</b>
FedMerDel_rand	2	84.1	94.8	<b>86.3</b>	65.2	54.8	38.6	90.1	56.0	67.3	47.8
FedMerDel_rand	3	<b>86.4</b>	95.4	85.8	73.9	47.6	34.6	<b>92.7</b>	63.0	64.4	49.4
FedMerDel_rand	4	81.4	<b>96.0</b>	83.8	71.7	51.7	<b>47.2</b>	92.5	67.7	<b>70.2</b>	44.8
FedMerDel_rand	5	82.7	94.6	83.4	<b>83.4</b>	<b>57.7</b>	34.5	92.0	<b>74.5</b>	52.4	34.7
FedMerDel_greedy	1	83.4	95.5	83.7	75.5	53.7	37.8	90.4	62.2	65.6	<b>51.4</b>
FedMerDel_greedy	2	84.1	94.8	<b>86.3</b>	70.2	54.8	33.6	90.1	56.0	64.5	47.8
FedMerDel_greedy	3	<b>86.4</b>	95.4	85.8	73.9	47.6	34.6	<b>92.7</b>	63.0	64.4	49.4
FedMerDel_greedy	4	81.4	<b>96.0</b>	83.8	71.7	51.7	<b>47.2</b>	92.5	67.7	<b>70.2</b>	44.8
FedMerDel_greedy	5	82.7	94.6	83.4	<b>83.4</b>	<b>57.7</b>	34.5	92.0	<b>74.5</b>	52.4	34.6
FedMerDel_30r	1	<b>91.8</b>	94.5	85.7	80.5	54.5	51.7	<b>94.3</b>	71.0	68.8	50.3
FedMerDel_30r	2	88.6	95.3	<b>85.8</b>	76.3	56.3	46.2	93.2	70.1	<b>69.0</b>	<b>59.7</b>
FedMerDel_30r	3	91.3	<b>95.4</b>	85.2	<b>83.0</b>	<b>59.8</b>	<b>53.8</b>	93.1	<b>78.5</b>	65.2	34.5
FedMerDel_30g	1	<b>91.8</b>	94.5	85.7	80.5	54.5	51.7	<b>94.3</b>	69.0	68.8	52.9
FedMerDel_30g	2	88.6	95.3	<b>85.8</b>	74.9	56.3	44.8	93.2	70.1	<b>71.6</b>	<b>59.7</b>
FedMerDel_30g	3	91.3	<b>95.4</b>	85.2	<b>84.2</b>	<b>62.4</b>	<b>53.8</b>	93.1	<b>76.9</b>	60.7	34.5
k-means_5_20		65.2	92.0	50.2	41.9	43.1	40.6	<b>86.9</b>	63.9	27.5	33.6
k-means_5_35		86.9	78.6	58.9	74.0	31.6	14.9	80.3	72.8	24.8	<b>56.5</b>
k-means_10_20		81.4	97.8	65.9	74.6	54.3	31.1	83.2	70.8	40.2	39.9
k-means_10_35		86.5	95.8	<b>73.5</b>	72.9	<b>77.6</b>	<b>43.4</b>	86.7	<b>81.2</b>	49.5	27.7
k-means_17_20		83.1	<b>98.6</b>	63.7	60.9	51.9	33.4	85.0	79.7	46.3	32.6
k-means_17_35		<b>91.5</b>	97.8	68.3	<b>77.9</b>	62.1	23.5	83.6	75.7	<b>57.0</b>	50.0
EM_20		82.1	95.6	83.7	84.9	<b>62.2</b>	29.7	91.8	72.4	57.4	38.0
EM_35		<b>87.6</b>	<b>96.1</b>	<b>90.2</b>	<b>85.8</b>	51.8	<b>51.9</b>	<b>94.8</b>	<b>81.8</b>	<b>72.3</b>	<b>62.6</b>
MCA_EM_20		74.9	87.5	<b>71.5</b>	46.2	53.7	<b>53.6</b>	87.0	41.2	0.00	<b>55.4</b>
MCA_EM_35		<b>81.7</b>	<b>89.8</b>	49.7	<b>73.1</b>	<b>58.9</b>	41.2	<b>89.1</b>	<b>62.7</b>	<b>19.3</b>	39.0



K.3. Generated Digits

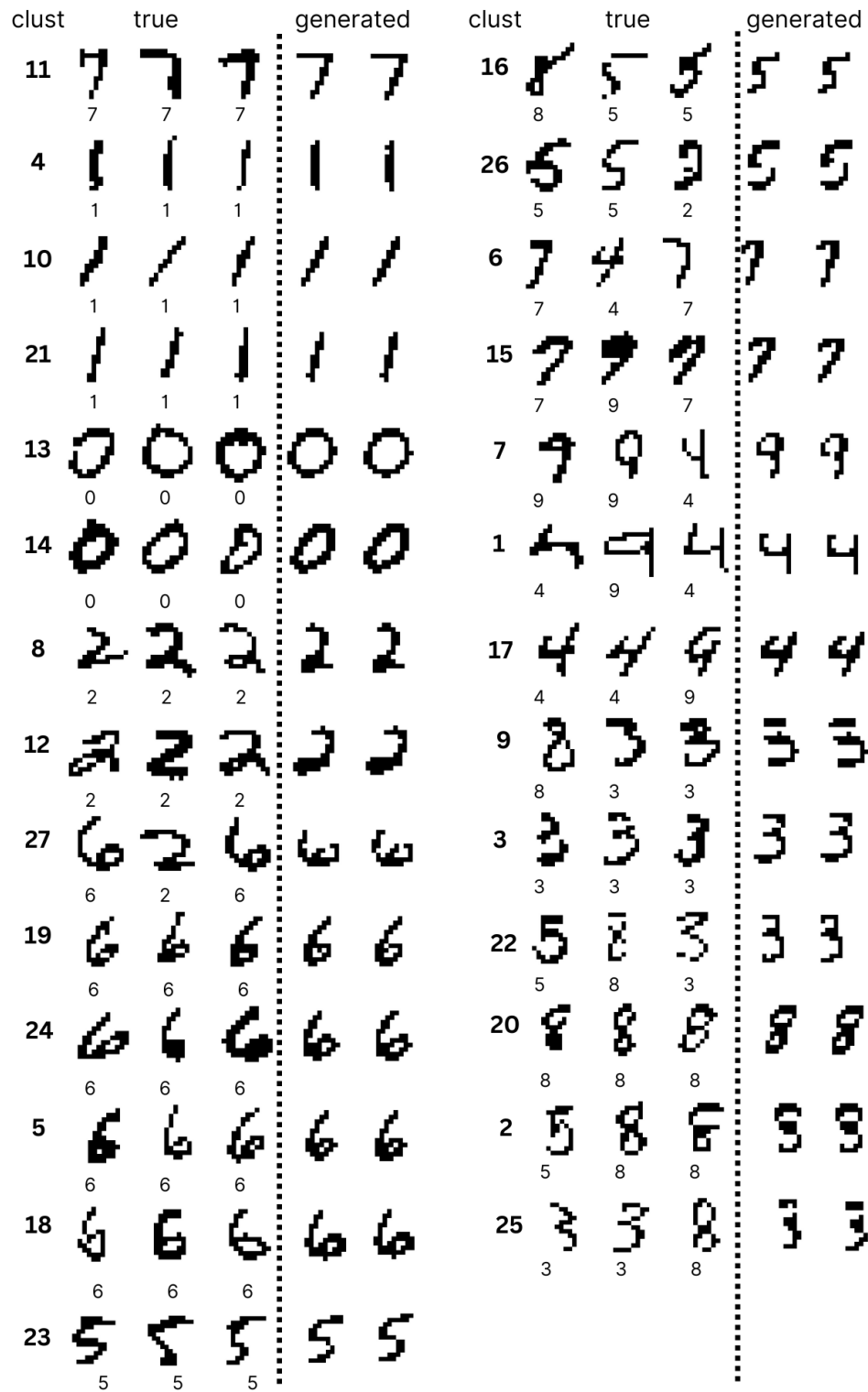


Figure S15. 3 randomly selected observations and 2 generated digits (from the variational distribution) from each cluster in the clustering model with the best ELBO for the MNIST data.

## L. EHR Data - Additional Information

EHR data were obtained from The Health Improvement Network database. The start date for our study was 01 January 2010 and end date was 01 January 2017. The dataset comprised primary care health data for 289,821 individuals over 80 years old who had at least two of the long term health conditions considered in our analysis. The full list of health conditions, and their coding, is provided in Table 20. 64.8% of individuals contributing to the analysis dataset were female, 35.2% were male.

### L.1. Greedy Search Global Merge

In Figure 3 of the main manuscript, we illustrated the global clusters identified using the “random search” approach to perform the global merge. In Figure S16 below, we provide the corresponding results obtained using the “greedy search” approach.

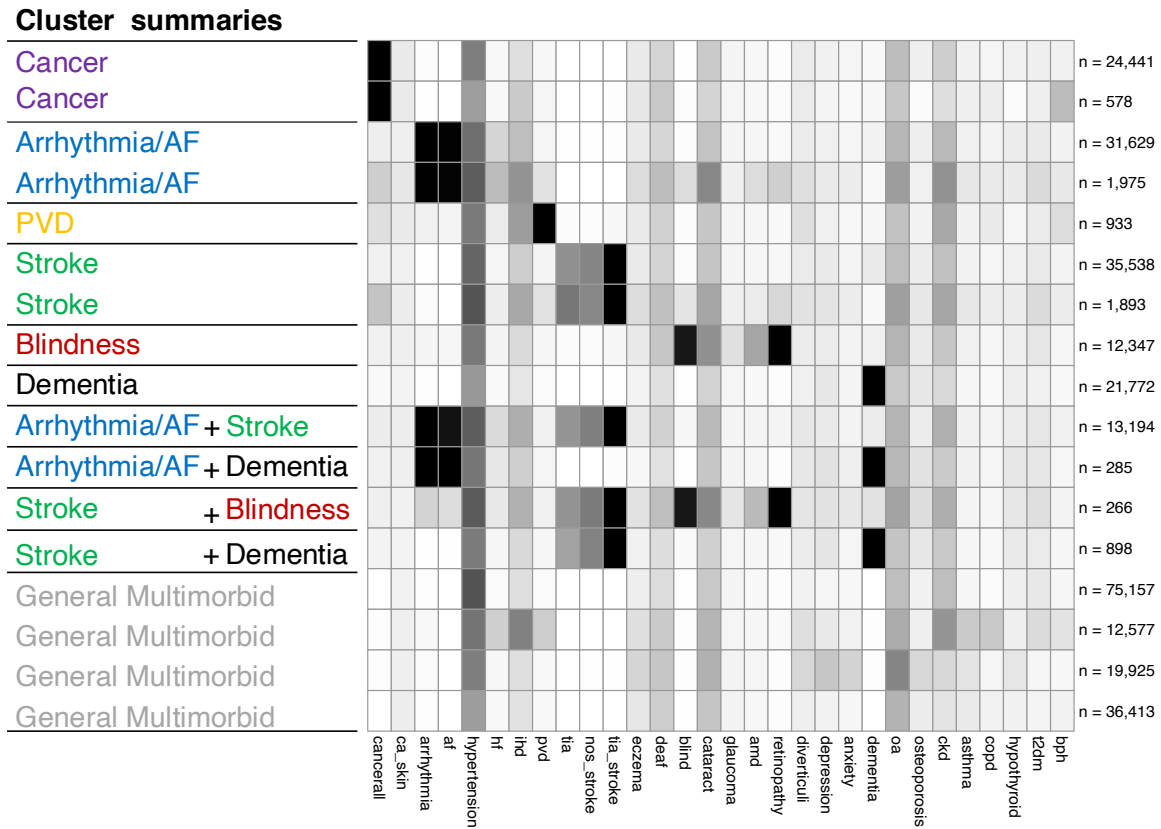


Figure S16. Results of global EHR clustering using the greedy search approach to perform the global merge. Columns are health conditions, and rows correspond to clusters. Row labels (shown on the right) indicate the number of individuals in each cluster. Summary names for each of the clusters are provided on the left of the plot. To improve visualisation, only the most prevalent health conditions are shown.

Table 20. Table providing the full list of health conditions, and their coding used in the analysis and figures.

Coding	Condition	Coding	Condition
cancerall	Any cancer diagnosis	endometriosis	Endometriosis
ca_lung	Lung cancer	pcos	Polycystic ovary syndrome
ca_breast	Breast cancer	pernicious_anaemia	Pernicious anaemia
ca_bowel	Bowel cancer	vte	Venous thromboembolism
ca_prostate	Prostate cancer	pulmonary_embolism	Pulmonary embolism
lymphoma	Lymphoma	coagulopathy	Coagulopathy
leukaemia	Leukaemia	depression	Depression
ca_skin	Skin cancer	anxiety	Anxiety
melanoma	Melanoma	smi	Serious mental illness
ca_metastatic	Metastatic cancer	substance_misuse	Substance misuse
arrhythmia	Arrhythmia	alcohol_problem	Alcohol problem
af	Atrial fibrillation	adhd	Attention deficit hyperactivity disorder
hypertension	Hypertension	eating_disorder	Eating disorder
hf	Hear failure	learning_disability	Learning disability
ihd	Ischemic heart disease	alzheimers	Alzheimer's diseases
valve_disease	Heart valve disease	vascular_dementia	Vascular dementia
cardiomyopathy	Cardiomyopathy	dementia	Dementia
con_heart_disease	Congenital heart disease	parkinsons	Pakinson's disease
pvd	Peripheral vascular disease	migraine	Migraine
aortic_aneurysm	Aortic aneurysm	ms	Multiple sclerosis
tia	Transient ischaemic attack	epilepsy	Epilepsy
isch_stroke	Ischaemic stroke	hemiplegia	Hemiplegia
haem_stroke	Haemorrhagic stroke	cfs	Chronic fatigue syndrome
nos_stroke	Stroke (not otherwise specified)	fibromyalgia	Fibromyalgia
tia_stroke	TIA stroke	oa	Osteoarthritis
eczema	Eczema	osteoporosis	Osteoporosis
psoriasis	Psoriasis	polymyalgia	Polymyalgia
vitiligo	Vitiligo	ra	Rheumatoid arthritis
alopecia	Alopecia	sjogren	Sjögren's syndrome
rhin_conjunc	Rhinoconjunctivitis	sle	Systemic lupus erythematosus
sinusitis	Sinusitis	systematic_sclerosis	Systematic sclerosis
deaf	Deafness	psoriatic_arthritis	Psoriatic arthritis
blind	Blindness	ank_spond	Ankylosing spondylitis
cataract	Cataract	gout	Gout
glaucoma	Glaucoma	ckd	Chronic kidney disease
amd	Age-related macular degeneration	copd	Chronic obstructive pulmonary disease
retinopathy	Retinopathy	asthma	Asthma
uveitis	Uveitis	osa	Obstructive sleep apnea
scleritis	Scleritis	bronchiectasis	Bronchiectasis
peptic_ulcer	Peptic ulcer	pulmonary_fibrosis	Pulmonary fibrosis
ibd	Inflammatory bowel disease	hyperthyroidism	Hyperthyroidism
ibs	Irritable bowel syndrme	hypothyroid	Hypothyroidism
liver_disease	Liver disease	t1dm	Type 1 diabetes mellitus
nash_nafl	Nonalcoholic steatohepatitis/ Non-alcoholic fatty liver	t2dm	Type 2 diabetes mellitus
diverticuli	Diverticulitis	hiv	Human immunodeficiency virus
coeliac	Coeliac disease	bph	Benign prostatic hyperplasia
pancreatitis	Pancreatitis	erectile_dysfunction	Erectile dysfunction